The precise physiological reasons for the evolution of these diverse pro-inflammatory gene activation pathways are not known. However, one important consequence is the capacity to regulate different subsets of genes with greater selectivity. Indeed, many of the primary response gene products may function properly only if activated rapidly and if produced at an appropriate level. For example, tumor necrosis factor-α and IL-1β are cytokines that trigger a series of inflammatory and host defense responses, and when produced in excess, they induce serious multiple organ failure (34). Other primary response gene products, the MIP-2 and GRO1 chemokines, mediate the recruitment of neutrophils during an acute phase of inflammation (35).

The rapid induction of many early primary response genes may therefore be of considerable benefit during the initiation of an immune response. At the same time, the need to overcome a nucleosome barrier may provide important benefits for secondary response genes, by allowing them to be activated with a higher degree of selectivity by different stimuli and in different biological scenarios. Consistent with this hypothesis, only a subset of secondary response genes require IκBζ for activation, whereas other transcription factors presumably carry out the same functions at other subsets of secondary response genes. In fact, our results provide evidence that the nucleosome barrier can confer a requirement for at least two transcription factors that are not generally required by early primary response genes. Therefore, at least one MyD88 target gene must be required for inducible nucleosome remodeling by SWI/SNF complexes, with IκBζ or its equivalent functioning at a later stage of the gene activation cascade to promote preinitiation complex assembly and histone H3K4 trimethylation. In this context, it is interesting to note that IκBζ-dependent secondary response gene products include cytokines and chemokines that are involved in the regulation of T cell-mediated immune responses; IL-12 p40 is a key subunit of the IL-12 and IL-23 heterodimeric cytokines, which are critical to Th1 and Th17 development, respectively (36), and IL-6 has recently been shown to be essential for initiation of Th17 cell development (37). Other IκBζ-dependent secondary response gene products, such as Ebi3, IL-18, and TARC (13), also regulate Th1/Th2/Th17 cell-mediated immune responses (38–42). Therefore, the nucleosome barrier for secondary response genes may have evolved to ensure tight regulation of adaptive immunity during TLR signaling.

Although the results of this analysis provide a framework toward understanding the differential regulation of pro-inflammatory genes, a number of important mechanistic questions remain to be answered. First, why is MyD88 required for primary response gene activation, despite the efficient recruitment of p65, TBP, and pol II to primary response promoters in *Myd88*$^{-/-}$ macrophages? A likely explanation is that these genes require a direct target of the MyD88 signaling pathway that remains to be characterized. However, an alternative is that the moderately delayed induction of NF-κB somehow disrupts transcriptional activation.

A second unanswered question is, what primary response gene products and MyD88 target genes are responsible for inducible remodeling at IκBζ-dependent secondary response genes, as well as other subsets of secondary response genes? This question has been especially difficult to answer. IκBζ appeared to be an ideal candidate because its regulatory functions are restricted to secondary response genes. However, we were unable to find evidence implicating IκBζ in the regulation of nucleosome remodeling. Analyses of several other primary response gene products for a possible role in the regulation of nucleosome remodeling at secondary response genes have also yielded negative results.[5] As an alternative to the candidate-gene approach, it may be possible to identify DNA sequence elements in secondary response promoters that are required for inducible nucleosome remodeling, which may lead to the critical transcription factors. However, it will first be necessary to develop an assay in which secondary response promoters assemble into a native chromatin structure that depends on a nucleosome remodeling event for transcriptional activation.

A third unanswered question is how IκBζ contributes to the recruitment of NF-κB p65 complexes, TBP, and pol II, and how it facilitates histone H3K4 trimethylation. A previous study provided evidence that IκBζ is recruited to target promoters by NF-κB p50 homodimers (13). One possibility is that the binding of p50 homodimers recruits IκBζ through a direct interaction, which then recruits a p65-containing dimer to a different NF-κB site, or to the same site through dimer exchange. The p65 dimer could then act in concert with other transcription factors bound to the promoter to recruit TBP and pol II and facilitate H3K4 trimethylation and transcription initiation. Other possible mechanisms of IκBζ function must also be considered, such as a direct role in the recruitment of an H3K4 methyltransferase.

The importance of chromatin for the differential regulation of TLR-dependent genes was recently highlighted in an elegant analysis of the negative regulation of the inflammatory response (18). Further dissection of the diverse mechanisms underlying these key regulatory events will help elucidate the molecular basis of immune disorders caused by abnormal activation of innate immunity.

Acknowledgments—We thank Y. Yamada and K. Takeda for technical assistance, T. Nakayama for helpful discussion, and M. Kurata and M. Yasuda for secretarial assistance.

REFERENCES

1. Akira, S., and Takeda, K. (2004) *Nat. Rev. Immunol.* **4,** 499–511
2. Iwasaki, A., and Medzhitov, R. (2004) *Nat. Immunol.* **5,** 987–995
3. Beutler, B., Jiang, Z., Georgel, P., Crozat, K., Croker, B., Rutschmann, S., Du, X., and Hoebe, K. (2006) *Annu. Rev. Immunol.* **24,** 353–389
4. Marshak-Rothstein, A. (2006) *Nat. Rev. Immunol.* **6,** 823–835
5. Liew, F. Y., Xu, D., Brint, E. K., and O'Neill, L. A. (2005) *Nat. Rev. Immunol.* **5,** 446–458
6. Negishi, H., Ohba, Y., Yanai, H., Takaoka, A., Honma, K., Yui, K., Matsuyama, T., Taniguchi, T., and Honda, K. (2005) *Proc. Natl. Acad. Sci. U. S. A.* **102,** 15989–15994
7. Kuwata, H., Matsumoto, M., Atarashi, K., Morishita, H., Hirotani, T., Koga, R., and Takeda, K. (2006) *Immunity* **24,** 41–51
8. Akira, S., Uematsu, S., and Takeuchi, O. (2006) *Cell* **124,** 783–801
9. Yamazaki, S., Muta, T., and Takeshige, K. (2001) *J. Biol. Chem.* **276,**

[5] V. Ramirez-Carrozzi and S. T. Smale, unpublished data.

27657–27662
10. Kitamura, H., Kanehira, K., Okita, K., Morimatsu, M., and Saito, M. (2000) *FEBS Lett.* **485,** 53–56
11. Haruta, H., Kato, A., and Todokoro, K. (2001) *J. Biol. Chem.* **276,** 12485–12488
12. Motoyama, M., Yamazaki, S., Eto-Kimura, A., Takeshige, K., and Muta, T. (2005) *J. Biol. Chem.* **280,** 7444–7451
13. Yamamoto, M., Yamazaki, S., Uematsu, S., Sato, S., Hemmi, H., Hoshino, K., Kaisho, T., Kuwata, H., Takeuchi, O., Takeshige, K., Saitoh, T., Yamaoka, S., Yamamoto, N., Yamamoto, S., Muta, T., Takeda, K., and Akira, S. (2004) *Nature* **430,** 218–222
14. Smale, S. T., and Fisher, A. G. (2002) *Annu. Rev. Immunol.* **20,** 427–462
15. Ansel, K. M., Lee, D. U., and Rao, A. (2003) *Nat. Immunol.* **4,** 616–623
16. Mostoslavsky, R., Alt, F. W., and Bassing, C. H. (2003) *Nat. Immunol.* **4,** 603–606
17. Natoli, G., Saccani, S., Bosisio, D., and Marazzi, I. (2005) *Nat. Immunol.* **6,** 439–445
18. Foster, S. L., Hargreaves, D. C., and Medzhitov, R. (2007) *Nature* **447,** 972–978
19. Roth, S. Y., Denu, J. M., and Allis, C. D. (2001) *Annu. Rev. Biochem.* **70,** 81–120
20. Lusser, A., and Kadonaga, J. T. (2003) *BioEssays* **25,** 1192–1200
21. Cairns, B. R. (2005) *Curr. Opin. Genet. Dev.* **15,** 185–190
22. de la Serna, I. L., Ohkawa, Y., and Imbalzano, A. N. (2006) *Nat. Rev. Genet.* **7,** 461–473
23. Li, B., Carey, M., and Workman, J. L. (2007) *Cell* **128,** 707–719
24. Bernstein, B. E., Humphrey, E. L., Erlich, R. L., Schneider, R., Bouman, P., Liu, J. S., Kouzarides, T., and Schreiber, S. L. (2002) *Proc. Natl. Acad. Sci. U. S. A.* **99,** 8695–8700
25. Martin, C., and Zhang, Y. (2005) *Nat. Rev. Mol. Cell Biol.* **6,** 838–849
26. Saccani, S., Pantano, S., and Natoli, G. (2001) *J. Exp. Med.* **193,** 1351–1359
27. Natoli, G. (2006) *FEBS Lett.* **580,** 2843–2849
28. Ramirez-Carrozzi, V. R., Nazarian, A. A., Li, C. C., Gore, S. L., Sridharan, R., Imbalzano, A. N., and Smale, S. T. (2006) *Genes Dev.* **20,** 282–296
29. Yamamoto, M., Sato, S., Hemmi, H., Hoshino, K., Kaisho, T., Sanjo, H., Takeuchi, O., Sugiyama, M., Okabe, M., Takeda, K., and Akira, S. (2003) *Science* **301,** 640–643
30. Weinmann, A. S., Plevy, S. E., and Smale, S. T. (1999) *Immunity* **11,** 665–675
31. Zhou, L., Nazarian, A. A., and Smale, S. T. (2004) *Mol. Cell. Biol.* **24,** 2385–2396
32. Santos-Rosa, H., Schneider, R., Bannister, A. J., Sherriff, J., Bernstein, B. E., Emre, N. C., Schreiber, S. L., Mellor, J., and Kouzarides, T. (2002) *Nature* **419,** 407–411
33. Bernstein, B. E., Kamal, M., Lindblad-Toh, K., Bekiranov, S., Bailey, D. K., Huebert, D. J., McMahon, S., Karlsson, E. K., Kulbokas, E. J., III, Gingeras, T. R., Schreiber, S. L., and Lander, E. S. (2005) *Cell* **120,** 169–181
34. Dinarello, C. A. (1991) *J. Infect. Dis.* **163,** 1177–1184
35. Zhang, X. W., Liu, Q., Wang, Y., and Thorlacius, H. (2001) *Br. J. Pharmacol.* **133,** 413–421
36. Trinchieri, G., Pflanz, S., and Kastelein, R. A. (2003) *Immunity* **19,** 641–644
37. Bettelli, E., Carrier, Y., Gao, W., Korn, T., Strom, T. B., Oukka, M., Weiner, H. L., and Kuchroo, V. K. (2006) *Nature* **441,** 235–238
38. Hunter, C. A. (2005) *Nat. Rev. Immunol.* **5,** 521–531
39. Batten, M., Li, J., Yi, S., Kljavin, N. M., Danilenko, D. M., Lucas, S., Lee, J., de Sauvage, F. J., and Ghilardi, N. (2006) *Nat. Immunol.* **7,** 929–936
40. Stumhofer, J. S., Laurence, A., Wilson, E. H., Huang, E., Tato, C. M., Johnson, L. M., Villarino, A. V., Huang, Q., Yoshimura, A., Sehy, D., Saris, C. J., O'Shea, J. J., Hennighausen, L., Ernst, M., and Hunter, C. A. (2006) *Nat. Immunol.* **7,** 937–945
41. Nakanishi, K., Yoshimoto, T., Tsutsui, H., and Okamura, H. (2001) *Annu. Rev. Immunol.* **19,** 423–474
42. Imai, T., Nagira, M., Takagi, S., Kakizaki, M., Nishimura, M., Wang, J., Gray, P. W., Matsushima, K., and Yoshie, O. (1999) *Int. Immunol.* **11,** 81–88

MyD88-Dependent Pathway in T Cells Directly Modulates the Expansion of Colitogenic CD4$^+$ T Cells in Chronic Colitis[1]

Takayuki Tomita,* Takanori Kanai,[2]* Toshimitsu Fujii,* Yasuhiro Nemoto,* Ryuichi Okamoto,* Kiichiro Tsuchiya,* Teruji Totsuka,* Naoya Sakamoto,* Shizuo Akira,† and Mamoru Watanabe*

TLRs that mediate the recognition of pathogen-associated molecular patterns are widely expressed on/in cells of the innate immune system. However, recent findings demonstrate that certain TLRs are also expressed in conventional TCR$\alpha\beta^+$ T cells that are critically involved in the acquired immune system, suggesting that TLR ligands can directly modulate T cell function in addition to various innate immune cells. In this study, we report that in a murine model of chronic colitis induced in RAG-2$^{-/-}$ mice by adoptive transfer of CD4$^+$CD45RB^{high} T cells, both CD4$^+$CD45RB^{high} donor cells and the expanding colitogenic lamina propria CD4$^+$CD44^{high} memory cells expresses a wide variety of TLRs along with MyD88, a key adaptor molecule required for signal transduction through TLRs. Although RAG-2$^{-/-}$ mice transferred with MyD88$^{-/-}$CD4$^+$CD45RB^{high} cells developed colitis, the severity was reduced with the delayed kinetics of clinical course, and the expansion of colitogenic CD4$^+$ T cells was significantly impaired as compared with control mice transferred with MyD88$^{+/+}$CD4$^+$CD45RB^{high} cells. When RAG-2$^{-/-}$ mice were transferred with the same number of MyD88$^{+/+}$ (Ly5.1$^+$) and MyD88$^{-/-}$ (Ly5.2$^+$) CD4$^+$CD45RB^{high} cells, MyD88$^{-/-}$CD4$^+$ T cells showed significantly lower proliferative responses assessed by in vivo CFSE division assay, and also lower expression of antiapoptotic Bcl-2/Bcl-x$_L$ molecules and less production of IFN-γ and IL-17, compared with the paired MyD88$^{+/+}$CD4$^+$ T cells. Collectively, the MyD88-dependent pathway that controls TLR signaling in T cells may directly promote the proliferation and survival of colitogenic CD4$^+$ T cells to sustain chronic colitis. ***The Journal of Immunology*****, 2008, 180: 5291–5299.**

Inflammatory bowel diseases (IBD)[3] are caused by excessive tissue damaging by chronic inflammatory responses in the gut wall, and commonly take persistent courses (1, 2). According to the present understanding, the diseases are caused by infiltrated colitogenic effector/memory CD4$^+$ T cells within the inflamed mucosa, which are presumably primed by commensal Ag-loading dendritic cells (DCs) in lymphoid tissues (3). However, the nature of colitogenic CD4$^+$ T cells over time during chronic colitis under the persistent presence of commensal bacteria remains largely unknown.

Importantly, it is well-known that experimental colitis does not develop when mice are kept in a germfree condition (4–6), suggesting that intestinal microflora are essential to initiate and maintain colitogenic CD4$^+$ T cells by stimuli through 1) TCR signaling by one or more commensal Ags (signal 1) and 2) TLR signaling by pathogen-associated molecular patterns (PAMPs) in addition to cytokines (signal 3) and costimulatory signaling (signal 2) (7, 8). However, there are no reports showing that TLR signaling directly stimulates colitogenic CD4$^+$ T cells for their proliferation and/or survival.

It is widely recognized that TLRs are expressed in/on the innate immune cells (9, 10), such as macrophages, DCs, and epithelial cells, and are crucially important primarily to activate these professional and nonprofessional APCs and secondarily promote T cell responses (11). However, accumulating evidence has shown that certain TLRs are also expressed on/in TCR$\alpha\beta^+$ T cells that are major acquired immune cell populations (12), suggesting that TLR signaling may possibly have some direct function on adaptive immunity. Hence, to assess the direct role of TLR signaling initiated by PAMPs of commensal bacteria in modulation of colitogenic CD4$^+$ T cell expansion during the development and the persistence of chronic colitis, we performed a series of adoptive transfer colitis experiments by transfer of CD4$^+$CD45RB^{high} T cells that are deficient for MyD88, a key adaptor molecule of TLR signaling (13, 14), into RAG-2$^{-/-}$ recipient mice whose TLR pathways remained intact throughout the innate immune system.

Materials and Methods

Animals

Six- to 10-wk-old Ly5.2-background (Ly5.2$^+$) MyD88$^{-/-}$ mice (13) were used. Ly5.2$^+$ C57BL/6 mice were purchased from Japan Clea. Ly5.1-background C57BL/6 mice and Ly5.2$^+$ C57BL/6 RAG-2$^{-/-}$ mice were obtained from Taconic Farms and Central Laboratories for Experimental Animals (Kawasaki, Japan). Mice were maintained under specific pathogen-free conditions in the Animal Care Facility of Tokyo Medical and Dental University (Tokyo, Japan). All experiments were approved by the

*Department of Gastroenterology and Hepatology, Graduate School, Tokyo Medical and Dental University, Tokyo, Japan; and †Department of Host Defense, Research Institute for Microbial Diseases, Osaka University, Osaka, Japan

Received for publication July 26, 2007. Accepted for publication February 16, 2008.

The costs of publication of this article were defrayed in part by the payment of page charges. This article must therefore be hereby marked *advertisement* in accordance with 18 U.S.C. Section 1734 solely to indicate this fact.

[1] This work was supported in part by Grants-in-Aid for Scientific Research, Scientific Research on Priority Areas, Exploratory Research and Creative Scientific Research from the Japanese Ministry of Education, Culture, Sports, Science, and Technology; the Japanese Ministry of Health, Labor, and Welfare; the Japan Medical Association; and Foundation for Advancement of International Science.

[2] Address correspondence and reprint requests to Dr. Takanori Kanai, Department of Gastroenterology and Hepatology, Graduate School, Tokyo Medical and Dental University, 1-5-45 Yushima, Bunkyo-ku, Tokyo 113-8519, Japan. E-mail address: taka.gast@tmd.ac.jp

[3] Abbreviations used in this paper: IBD, inflammatory bowel disease; DC, dendritic cell; PAMP, pathogen-associated molecular pattern; PB, peripheral blood; SP, spleen; MLN, mesenteric lymph node; BM, bone marrow; WT, wild type; LP, lamina propria; IEL, intraepithelial cell; HPF, high-power field.

 0022-1767/08/$2.00

regional animal study committees and were done according to institutional guidelines and Home Office regulations.

Purification of T cell subsets

For isolation of peripheral blood (PB) lymphocytes, 600 μl of PB was collected from each mouse and was diluted 1/1 with PBS. The diluted PB was layered over Lymphosepar II (IBL) and centrifuged at 400 × *g* for 30 min at room temperature. Lymphocytes were then isolated from the plasma-Ficoll interface. Spleen (SP) and mesenteric lymph nodes (MLN) were mechanically disrupted into single-cell suspensions. Bone marrow (BM) was collected from the femur by flushing with sterile PBS.

CD4$^+$ T cells were isolated from SP cells of MyD88$^{-/-}$ and littermate MyD88$^{+/+}$ mice using the anti-CD4 (L3T4)-MACS system (Miltenyi Biotec) according to the manufacturer's instruction. Enriched CD4$^+$ T cells (94–96% pure, as estimated by FACSCalibur; BD Biosciences) were then labeled with PE-conjugated anti-mouse CD4 (RM4-5; BD Pharmingen) and FITC-conjugated anti-CD45RB (16A; BD Pharmingen). The subpopulation of CD4$^+$CD45RB^{high} cells was collected by two-color sorting on a FACS Aria (BD Biosciences), and was >98.0% pure on reanalysis.

To obtain LP CD4$^+$ T cells, colitis was induced in RAG-2$^{-/-}$ mice by adoptive transfer of CD4$^+$CD45RB^{high} T cells either from MyD88$^{-/-}$ or from littermate wild-type (WT) MyD88$^{+/+}$ mice as described previously (15). Colitic CD4$^+$CD45RB^{high} T cell-transferred RAG-2$^{-/-}$ mice were sacrificed at 6–10 wk after transfer. The entire colon was opened longitudinally, washed with PBS, and cut into small pieces. The dissected mucosa was incubated with Ca^{2+}, Mg^{2+}-free HBSS containing 1 mM DTT (Sigma-Aldrich) for 45 min to remove mucus and then treated with 2.0 mg/ml collagenase (Roche) and 0.01% DNase (Worthington Biomedical) for 2 h. The cells were pelleted twice through a 40% isotonic Percoll solution, and then subjected to Ficoll-Hypaque density gradient centrifugation (40%/75%). Enriched lamina propria (LP) CD4$^+$ T cells were obtained by positive selection using anti-CD4 (L3T4) MACS magnetic beads. The resultant cells contained >95% CD4$^+$ cells when analyzed by FACSCalibur. To assess the expression of TLRs and MyD88 in CD4$^+$ T cells using RT-PCR, every cell population was isolated by FACS Aria (BD Biosciences) to gain >98% CD4$^+$ purity.

RT-PCR

Total RNA was isolated by using Isogen reagent (Nippon Gene). Aliquots of total RNA (0.5 μg) were used for cDNA synthesis in a 20-μl reaction volume using random primers. One microliter of reverse transcription product was amplified with 0.25 U of rTaq DNA polymerase (Toyobo) in a 25-μl reaction. Sense and antisense primers and the cycle numbers for the amplification of each gene (16) were as follows: TLR1, sense 5′-TCTCT GAAGGCTTTGTCGATACA-3′ and antisense 5′-GACAGAGCCTGTA AGCATATTCG-3′ (35 cycles); TLR2, sense 5′-TCTAAAGTCGATC CGCGACAT-3′ and antisense 5′-TACCCAGCTCGCTCACTACGT-3′ (35 cycles); TLR3, sense 5′-TTGTCTTCTGCACGAACCTG-3′ and antisense 5′-CGCAACGCAAGGATTTTATT-3′ (35 cycles); TLR4, sense 5′-CAAGAACATAGATCTGAGCTTCAACCC-3′ and antisense 5′-GCT GTCCAATAGGGAAGCTTTCTAGAG-3′ (35 cycles); TLR5, sense 5′-ACTGAATTCCTTAAGCGACGTA-3′ and antisense 5′-AGAAGATAA AGCCGTGCGAAA-3′ (35 cycles); TLR6, sense 5′-AACAGGATAC GGAGCCTTGA-3′ and antisense 5′-CCAGGAAAGTCAGCTTCGTC-3′ (35 cycles); TLR7, sense 5′-TTCCGATACGATGAATATGCACG-3′ and antisense 5′-TGAGTTTGTCCAGAAGCCGTAAT-3′ (35 cycles); TLR8, sense 5′-GGCACAACTCCCTTGTGATT-3′ and antisense 5′-CATTTG GGTGCTGTTGTTTG-3′ (35 cycles); TLR9, sense 5′-CCGCAAGA CTCTATTTGTGCTGG-3′ and antisense 5′-TGTCCCTAGTCAGG GCTGTACTCAG-3′ (35 cycles); MyD88, sense 5′-GGCCTTGTTAGA CCGTGAGG-3′ and antisense 5′-TCATCTTCCCCTCTGCCCTA-3′ for (35 cycles); β-actin, sense 5′-GTGGGCCGCTCTAGGCACCAA-3′ and antisense 5′-CTCTTTGATGTCACGCACGATTTC-3′ (30 cycles). PCR products were separated on 1.8% agarose gels, stained with ethidium bromide, and visualized with a Lumi-Imager F1 (Roche Diagnostics).

Quantitative PCR

To validate gene expression changes, quantitative RT-PCR analysis was performed by Applied Biosystems 7500 using validated TaqMan Gene Expression Assays (Applied Biosystems). The TaqMan probes and primers for mouse Bcl-2 (assay identification number Mm00477631_m1) and mouse Bcl-x_L (assay identification number Mm00437783_m1) were Assay-on-Demand gene expression products (Applied Biosystems). The mouse β-actin gene was used as endogenous control (catalog number 4352933E; Applied Biosystems). The thermal cycler conditions were as follows: hold for 10 min at 95°C, followed a cycle of 95°C for 15 s and 60°C for 1 min for 45 cycles. All samples were performed in triplicate.

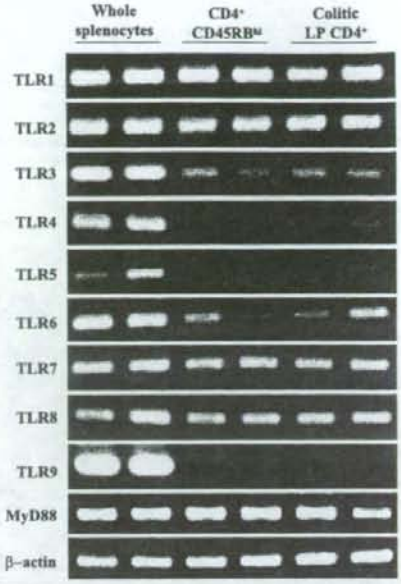

FIGURE 1. CD4$^+$CD45RB^{high} donor cells and colitic LP CD4$^+$ T cells express mRNAs for TLR and MyD88. Splenocytes and CD4$^+$CD45RB^{high} T cells from normal C57BL/6 mice, or LP CD4$^+$ T cells from colitic RAG-2$^{-/-}$ mice transferred with CD4$^+$CD45RB^{high} T cells, were strictly isolated using FACSAria (purity, >98.0%) and subjected for total RNA extraction. The RNA was reverse transcripted and amplified with gene for specific primers. PCR products were separated by agarose gel electrophoresis and stained with ethidium bromide. All the RT-PCR experiments were performed at least three times on independent samples.

Amplification data were analyzed with an Applied Biosystems Sequence Detection Software version 1.3. The relative expression of the gene of interest was normalized by the expression of β-actin.

In vivo experimental design

We performed a series of in vivo transfer experiments to investigate the role of TLR signaling in CD4$^+$CD45RB^{high} T cells or in colitogenic LP CD4$^+$ T cells in the development and persistence of murine chronic colitis.

Experiment 1. To assess the requirement of MyD88-dependent signaling in the development of colitis including the processes for T cell priming and activation, along with the persistence of colitogenic effector or memory CD4$^+$ T cells, we performed a cell transfer experiment using MyD88$^{-/-}$ and littermate WT MyD88$^{+/+}$ mice as donors. CD4$^+$CD45RB^{high} T cells from MyD88$^{-/-}$ ($n = 6$) or MyD88$^{+/+}$ ($n = 6$) donors were injected i.p. into RAG-2$^{-/-}$ mice and the recipients were monitored for 4–6 wk after transfer. In another set of experiment using the present protocol, we monitored the groups of mice (each $n = 5$) to 10 wk after transfer to assess the kinetics of the development.

Experiment 2. To further assess the necessity of MyD88-dependent signaling in the development of colitis, we performed in vivo competition experiments. The same number (2.5×10^5 cells/mouse) of CD4$^+$CD45RB^{high} T cells from MyD88$^{+/+}$ (Ly5.1$^+$) or MyD88$^{-/-}$ (Ly5.2$^+$) mice were coinjected i.p. into RAG-2$^{-/-}$ mice ($n = 6$), and the recipients were monitored for 6 wk after transfer.

Experiment 3. To assess the requirement of MyD88-dependent signaling for the persistence of colitogenic memory CD4$^+$ T cells in this CD4$^+$CD45RB^{high} T cell-transferred colitis model, independently from the impact of naive T cell priming, activation, and differentiation, we performed the adoptive retransfer of colitogenic LP memory CD4$^+$ T cells derived from colitic mice that were transferred with CD4$^+$CD45RB^{high} T cells of either MyD88$^{+/+}$ ($n = 6$) or MyD88$^{-/-}$ mice ($n = 6$) after 10 wk from transfer (17).

Experiment 4. To further assess the requirement of MyD88-dependent signaling for the persistence of colitogenic memory CD4$^+$ T cells, we

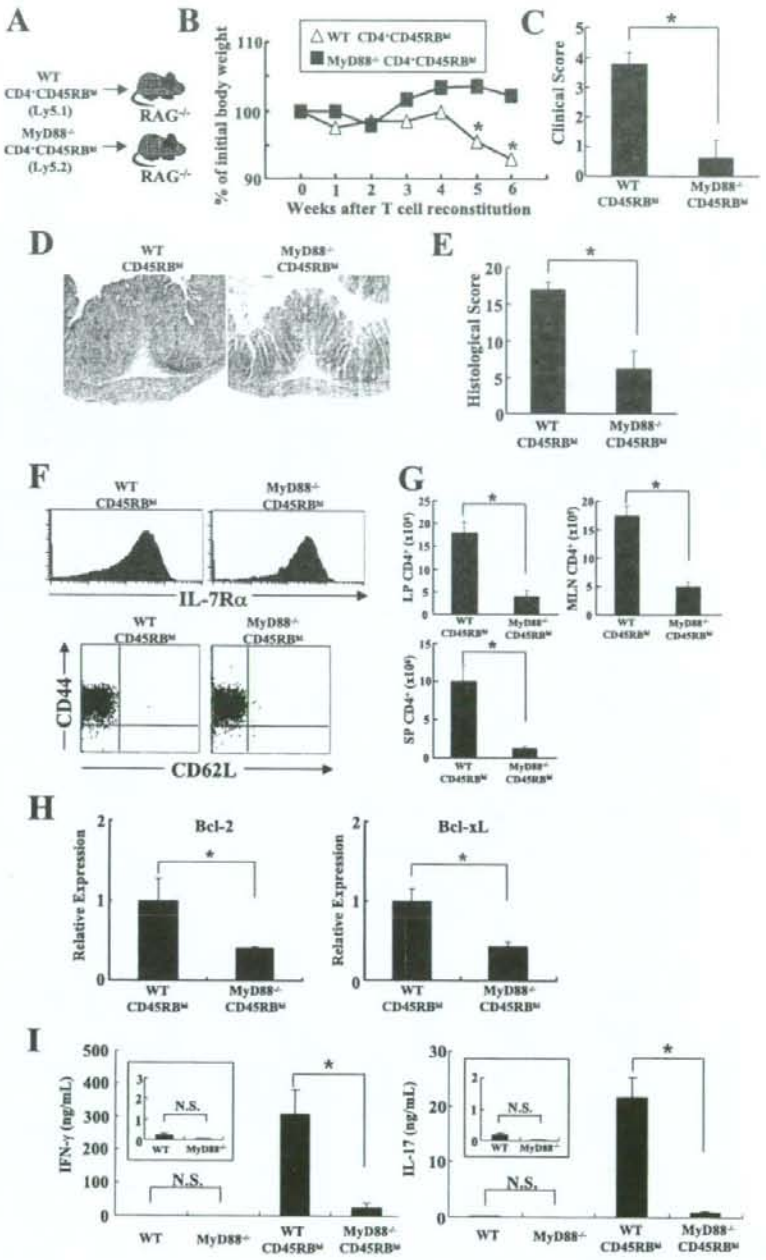

FIGURE 2. RAG-2$^{-/-}$ mice transferred with MyD88$^{-/-}$ CD4$^+$CD45RB^{high} T cells develop milder colitis. *A*, RAG-2$^{-/-}$ mice were transferred with splenic MyD88$^{+/+}$ (WT) ($n = 6$) or MyD88$^{-/-}$ ($n = 6$) CD4$^+$CD45RB^{high} T cells (3×10^5 cells/mouse). *B*, Change in body weight over time is expressed as percent of the original weight. Data are represented as the mean ± SEM of six mice in each group. *, $p < 0.05$. *C*, Clinical scores were determined at 6 wk after transfer as described in *Materials and Methods*. Data are indicated as mean ± SEM of six mice in each group. *, $p < 0.01$. *D*, Histological examination of the colon from WT (*left*) or MyD88$^{-/-}$ (*right*) CD4$^+$CD45RB^{high} T cells at 6 wk after transfer. Original magnification, ×100. *E*, Histological scoring of mice transferred with WT or MyD88$^{-/-}$CD4$^+$CD45RB^{high} T cells at 6 wk after transfer. Data are indicated as mean ± SEM of six mice in each group. *, $p < 0.01$. *F*, Phenotypic characterization of LP CD4$^+$ T cells isolated from mice transferred with WT or MyD88$^{-/-}$CD4$^+$CD45RB^{high} T cells at 6 wk after transfer. *G*, LP, MLN, and SP CD4$^+$ T cells were isolated from mice transferred with WT or MyD88$^{-/-}$ CD4$^+$CD45RB^{high} T cells at 6 wk after transfer, and the number of CD4$^+$ cells was determined by flow cytometry. Data are indicated as mean ± SEM of six mice in each group. *, $p < 0.01$. *H*, Expression of Bcl-2 and Bcl-x_L mRNAs in SP cells was determined by quantitative RT-PCR, and are shown as relative amount of indicated mRNA normalized by expression of β-actin. Data are represented as the mean ± SEM of six samples. *, $p < 0.05$. *I*, Cytokine production by LP CD4$^+$ T cells. LP CD4$^+$ T cells were isolated at 6 wk after transfer and stimulated with anti-CD3 and anti-CD28 mAbs for 48 h. IFN-γ and IL-17 concentrations in culture supernatants were measured by ELISA. Data are indicated as mean ± SEM of six mice in each group. *, $p < 0.01$. WT; healthy WT mice, MyD88$^{-/-}$; healthy MyD88$^{-/-}$ mice, WT CD45RB^{high}; RAG-2$^{-/-}$ mice transferred with WT CD4$^+$CD45RB^{high} T cells, MyD88$^{-/-}$CD45RB^{high}; RAG-2$^{-/-}$ mice transferred with MyD88$^{-/-}$CD4$^+$ CD45RB^{high} T cells.

performed in vivo competition experiments. The same number (2.0×10^5 cells/mouse) of colitogenic LP memory CD4$^+$ T cells obtained from colitic mice that were transferred with either MyD88$^{+/+}$ (Ly5.1$^+$) or MyD88$^{-/-}$ (Ly5.2$^+$) CD4$^+$CD45RB^{high} T cells from either MyD88$^{+/+}$ mice (Ly5.1$^+$) or MyD88$^{-/-}$ mice (Ly5.2$^+$) after 10 wk from transfer were coinjected i.p. into new RAG-2$^{-/-}$ mice ($n = 6$), and the mice were monitored for 6 wk after the retransfer.

In experiments 1–4, all mice were assessed for a clinical score (18) that is the sum of four parameters listed as follows: hunching and wasting, 0 or 1; colon thickening, 0–3 (0, no colon thickening; 1, mild thickening; 2, moderate thickening; 3, extensive thickening); and stool consistency, 0–3 (0, normal beaded stool; 1, soft stool; 2, diarrhea; 3, bloody stool) (18). To monitor the clinical sign during the observed period over time, the ongoing disease activity index is defined as the sum (0–5 points) of the above-mentioned parameters except the colon thickening.

Experiment 5. To assess the requirement of MyD88-dependent signaling for the lymphopenia-driven rapid proliferation (19) of colitogenic memory CD4$^+$ T cells, we performed a short-term observation of in vivo competition experiments in combination with the CFSE-labeling method. The same number (2.0×10^6 cells/mouse) of CFSE-labeled LP memory CD4$^+$ T cells from colitic mice that were initially transferred with MyD88$^{+/+}$ (Ly5.1$^+$) or MyD88$^{-/-}$ (Ly5.2$^+$) CD4$^+$CD45RB^{high} T cells at 10 wk after transfer were injected i.p. into new RAG-2$^{-/-}$ mice ($n = 6$). In experiment 5, mice were sacrificed 10 days after retransfer, and assessed for cell divisions by CFSE dilution.

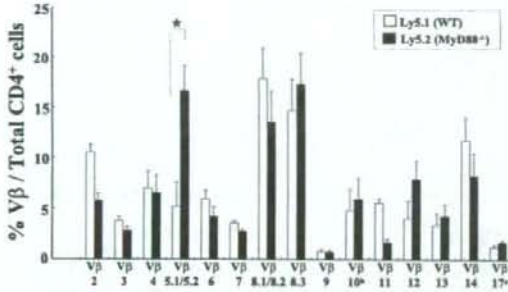

FIGURE 3. Vβ repertoire shows little difference between MyD88$^{+/+}$ or MyD88$^{-/-}$ donor cells. To analyze the TCR Vβ family repertoire, SP cells were isolated from mice transferred with Ly5.1$^+$MyD88$^{+/+}$ (WT) or Ly5.2$^+$MyD88$^{-/-}$CD4$^+$CD45RB^{high} T cells at 6 wk after transfer, and then triple-stained with PerCP-conjugated ant-CD3ε mAb (145-2C11), PE-conjugated anti-CD4 mAb (RM4-5), and a panel of 15 FITC-conjugated Vβ mAbs. Each percentage value indicates the frequency of each Vβ pooled from three independent experiments ($n = 6$). *, $p < 0.05$.

Histological examination

Tissue samples were fixed by 10% neutral-buffered formalin, and paraffin-embedded sections (5 μm) were stained with H&E. Three tissue samples from the proximal, middle, and distal parts of the colon were prepared and subjected for analysis. The sections were analyzed without prior knowledge of the type of T cell reconstitution. The most affected area was graded by the severity of lesions. The degree of colonic inflammation was calculated using a previous scoring system (20): mucosa damage, 0; normal, 1; 3–10 intraepithelial cells (IEL)/high power field (HPF) and focal damage, 2; >10 IEL/HPF and rare crypt abscesses, 3; >10 IEL/HPF, multiple crypt abscesses and erosion/ulceration, submucosa damage, 0; normal or widely scattered leukocytes, 1; focal aggregates of leukocytes, 2; diffuse leukocyte infiltration with expansion of submucosa, 3; diffuse leukocyte infiltration, muscularis damage, 0; normal or widely scattered leukocytes, 1; widely scattered leukocyte aggregates between muscle layers, 2; leukocyte infiltration with focal effacement of the muscularis, 3; extensive leukocyte infiltration with transmural effacement of the muscularis.

Cytokine ELISA

To measure cytokine production, 1×10^5 LP CD4$^+$ T cells were cultured in 200 μl of culture medium at 37°C in a humidified atmosphere containing 5% CO_2, using 96-well plates (Costar) which were precoated with 5 μg/ml hamster anti-mouse CD3ε mAb (145-2C11; BD Pharmingen) and hamster 2 μg/ml anti-mouse CD28 mAb (37.51; BD Pharmingen) in PBS overnight at 4°C. Culture supernatants were removed after 48 h and assayed for cytokine production. Cytokine concentrations were determined by specific ELISA following the manufacturer's recommendation (R&D Systems).

Flow cytometry

To detect the surface expression of molecules, isolated splenocytes, MLN, PB, BM, or LP mononuclear cells were preincubated with an FcγR-blocking mAb (CD16/32; 2.4G2; BD Pharmingen) for 15 min followed by incubation with specific FITC-, PE-, PerCP-, allophycocyanin- or biotin-labeled Abs for 20 min on ice. The following mAbs except biotin-conjugated anti-mouse IL-7Rα (A7R34; eBioscience) were obtained from BD Pharmingen; anti-CD3ε mAb (145-2C11), anti-CD4 mAb (RM4-5), anti-CD45RB mAb (16A), anti-CD62L (MEL-14), anti-CD44 mAb (IM7), anti-CD69 mAb (H1.2F3). Biotinylated Abs were detected with PE-streptavidin. Standard three- or four-color flow cytometric analysis was performed by the FACSCalibur equipped with CellQuest software. Background fluorescence was assessed by the staining of control irrelevant isotype. To analyze the TCR Vβ family repertoire, splenic cells were triple-stained with PerCP-conjugated anti-CD3ε mAb (145C-11), PE-conjugated anti-CD4 mAb (RM4-5), and either of the following FITC-conjugated mAbs: Vβ2; KJ25, Vβ3; KT4, Vβ4; MR9-4, Vβ5.1/5.2; RR4-7, Vβ6; TR310, Vβ7; MR5-2, Vβ8.1/2; B21.14, Vβ8.3; MR10-2, Vβ9; B21.5, Vβ10^b; RR3-15, Vβ11; MR11-1, Vβ12; IN12.3, Vβ13; 14.2, Vβ14; and KJ23, Vβ17^a. All the Abs were purchased from BD Pharmingen.

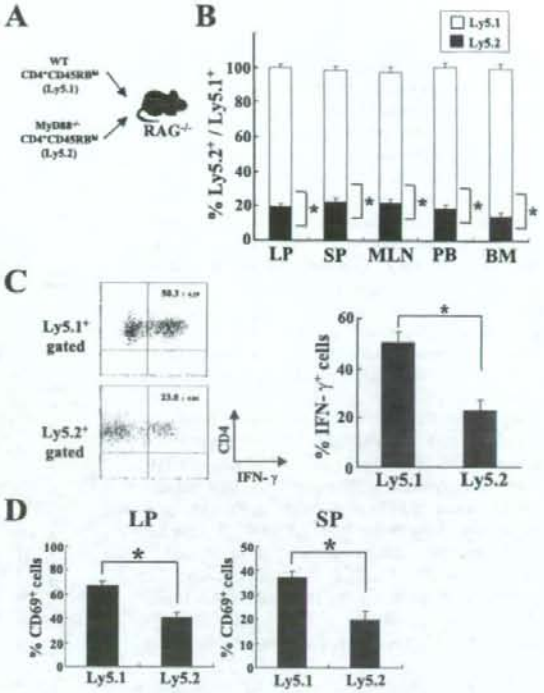

FIGURE 4. Expansive activity of MyD88$^{+/+}$ donor cells predominates over that of MyD88$^{-/-}$ donor cells in an in vivo competition assay. *A*, The same number (2.5×10^5 cells/mouse) of CD4$^+$CD45RB^{high} T cells from Ly5.1$^+$MyD88$^{+/+}$ (WT) mice and Ly5.2$^+$MyD88$^{-/-}$ mice was coinjected i.p. into RAG-2$^{-/-}$ mice ($n = 6$). *B*, Six weeks after transfer, LP, SP, MLN, PB, and BM CD4$^+$ T cells were isolated, and the ratio of Ly5.1$^+$ and Ly5.2$^+$ CD4$^+$ cells was determined by flow cytometry. *, $p < 0.01$. *C*, The frequencies of IFN-γ-producing LP CD4$^+$ T cells per total Ly5.1$^+$ or Ly5.2$^+$ cells were analyzed in the indicated subpopulations by flow cytometry. Data are represented as mean ± SEM of three independent experiments. *, $p < 0.01$. *D*, Phenotypic characterization of LP and SP CD4$^+$ T cells after transfer of CD4$^+$CD45RB^{high} T cells. % CD69$^+$, Percentages of CD4$^+$CD69$^+$ cells per total CD4$^+$ cells. Data are represented as mean ± SEM of six mice per group. *, $p < 0.05$.

CFSE labeling of T cells

T cell division in vivo was assessed by flow cytometry of CFSE-labeled cells. Isolated LP CD4$^+$ T cells were stained in vitro with the cytoplasmic dye CFSE (Molecular Probes) before reconstitution by incubation for 10 min at 37°C with 5 μM CFSE. The labeling reaction was quenched by washing in ice-cold RPMI 1640 supplemented with 10% FCS.

Statistical analysis

The results are expressed as mean ± SEM. Groups of data were compared by Mann-Whitney *U* test. Differences in data were considered to be statistically significant when $p < 0.05$.

Results

TLRs are expressed in CD4$^+$CD45RB^{high} donor cells and colitic LP CD4$^+$ cells

To assess the direct involvement of TLR signaling in regulating cell function of CD4$^+$ T cells composing chronic colitis under the presence of commensal bacteria, we examined whether mRNAs of TLR1–9 and their adaptor molecule, MyD88, are expressed in donor T cells or the LP CD4$^+$ T cells in colitic RAG-2$^{-/-}$ mice transferred with CD4$^+$CD45RB^{high} T cells. To do so, we isolated

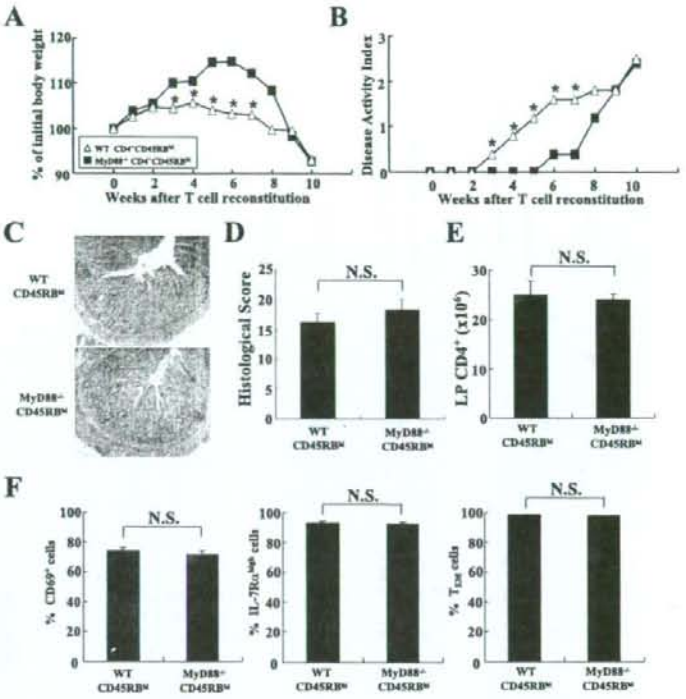

FIGURE 5. RAG-2$^{-/-}$ mice transferred with MyD88$^{-/-}$CD4$^+$CD45RB^{high} T cells develop colitis with the delayed kinetics, but reach to a similar level of mice transferred with MyD88$^{+/+}$CD4$^+$CD45RB^{high} T cells at 10 wk after transfer. *A*, Change in body weight is expressed as the percent of the original weight. Data are represented as mean ± SEM of five mice in each group. *, $p < 0.05$. WT, MyD88$^{+/+}$. *B*, Ongoing disease activity index was monitored during the course. Data are indicated as mean ± SEM of five mice in each group. *, $p < 0.05$. *C*, Histological examination of the colon from WT (*upper*) or MyD88$^{-/-}$ (*lower*) CD4$^+$CD45RB^{high} T cells at 10 wk after transfer. Original magnification, ×100. *D*, Histological scoring of mice transferred with WT or MyD88$^{-/-}$CD4$^+$CD45RB^{high} T cells at 10 wk after transfer. Data are indicated as the mean ± SEM of five mice in each group. *E*, LP CD4$^+$ T cells were isolated from mice transferred with WT or MyD88$^{-/-}$CD4$^+$CD45RB^{high} T cells at 10 wk after transfer, and the number of CD4$^+$ cells was determined by flow cytometry. Data are indicated as mean ± SEM of five mice in each group. *F*, Phenotypic characterization of LP CD4$^+$ T cells isolated from mice transferred with WT or MyD88$^{-/-}$CD4$^+$CD45RB^{high} T cells at 10 wk after transfer. The percentage of positive cells per total CD4$^+$ T cells (CD69$^+$/CD4$^+$, IL-7Rα$^+$/CD4$^+$, CD4$^+$CD44^{high} CD62L$^-$/CD4$^+$) was determined using flow cytometry.

each CD4$^+$ population under highly stringent gate definitions using FACSAria to avoid contamination of cells, such as macrophages, DCs, and B cells. As shown by RT-PCR in Fig. 1, whole splenocytes including T cells, B cells, macrophages, and DCs were used as the positive control, and expressed all members of TLR1–9 and MyD88. Under this condition, CD4$^+$CD45RB^{high} donor cells expressed MyD88 and TLRs except TLR-4, 5, and 9 along with MyD88, while colitic LP CD4$^+$ T cells expressed all members of TLRs and MyD88, indicating that TLR signaling via MyD88 may be directly involved in the priming, activation, proliferation, and survival of CD4$^+$ T cells in the present transfer model. The data were further by completely no detection of PCR products from a template prepared without the addition of reverse transcriptase, excluding a possibility of signals derived from contaminating genomic DNA rather than mRNA (data not shown).

RAG-2$^{-/-}$ mice transferred with MyD88$^{-/-}$CD4$^+$CD45RB^{high} T cells developed milder colitis

To explore whether the MyD88-signaling pathway in T cells is involved in the development of chronic colitis, we transferred MyD88$^{-/-}$ or MyD88$^{+/+}$ CD4$^+$CD45RB^{high} T cells into RAG-2$^{-/-}$ (MyD88$^{+/+}$) recipient mice maintaining an intact MyD88-dependent pathway of the innate immune system, meaning that only the transferred CD4$^+$ T cells lack the MyD88-dependent pathway within the recipient mice (Fig. 2*A*). When WT MyD88$^{+/+}$ CD4$^+$CD45RB^{high} cells were transferred into RAG-2$^{-/-}$ mice, the recipients rapidly developed severe wasting disease associated with clinical signs of severe colitis. Particularly, weight loss (Fig. 2*B*), persistent diarrhea and also occasionally bloody stool or anal prolapse was observed by tracking the clinical score up to 6 wk after transfer (Fig. 2*C*). However, when MyD88$^{-/-}$CD4$^+$ CD45RB^{high} T cells were transferred into RAG-2$^{-/-}$ mice, the recipients also developed wasting disease and colitis despite the delayed onset (see the following result in Fig. 5), but the clinical score at 6 wk after transfer was significantly lower as compared with that of mice transferred with control MyD88$^{+/+}$ CD4$^+$CD45RB^{high} T cells (Fig. 2*C*). Thus, the delayed onset and milder clinical score of mice transferred with MyD88$^{-/-}$CD4$^+$ CD45RB^{high} cells would easily be explained by the lack of a MyD88-dependent pathway in donor CD4$^+$ T cells, but not in other innate immune cells of the recipient mice.

At 6 wk after transfer, the colon from of mice transferred with MyD88$^{+/+}$ donor cells, but not that from mice transferred with MyD88$^{-/-}$ donor cells, was enlarged and had a greatly thickened wall (data not shown). In addition, the enlargement of the SP and MLN was also present in mice transferred with MyD88$^{+/+}$ donor cells as compared with mice transferred with MyD88$^{-/-}$ donor cells (data not shown). Histological examination revealed that mice transferred with MyD88$^{+/+}$ donor cells developed severe colitis showing prominent epithelial hyperplasia and erosion with a massive infiltration of mononuclear cells in LP of the colon (Fig. 2*D*). In contrast, mice transferred with MyD88$^{-/-}$ donor cells developed milder colitis as compared with mice transferred with MyD88$^{+/+}$ donor cells. This difference was statistically confirmed by histological scoring of multiple colon sections, which was mice transferred with MyD88$^{+/+}$ donor cells, 17.0 ± 1.0; and mice transferred with MyD88$^{-/-}$ donor cells, 6.2 ± 2.42 ($p < 0.01$) (Fig. 2*E*). Importantly, flow cytometry analysis revealed that the LP CD4$^+$ T cells isolated from recipients transferred with either MyD88$^{-/-}$ or MyD88$^{+/+}$ CD4$^+$CD45RB^{high} T cells were CD44^{high}CD62L$^-$IL-7Rα^{high} (Fig. 2*F*), indicating that the transferred CD4$^+$CD45RB^{high} T cells could differentiate into effector-memory T cells even in the absence of the MyD88-dependent pathway within colitic CD4$^+$ T cells.

A further quantitative evaluation of CD4$^+$ T cell infiltration was made by isolating LP, MLN, and SP CD3$^+$CD4$^+$ T cells. As shown in Fig. 2*G*, significantly lower numbers of CD4$^+$ T cells were recovered from LP, MLN, and SP of mice transferred with

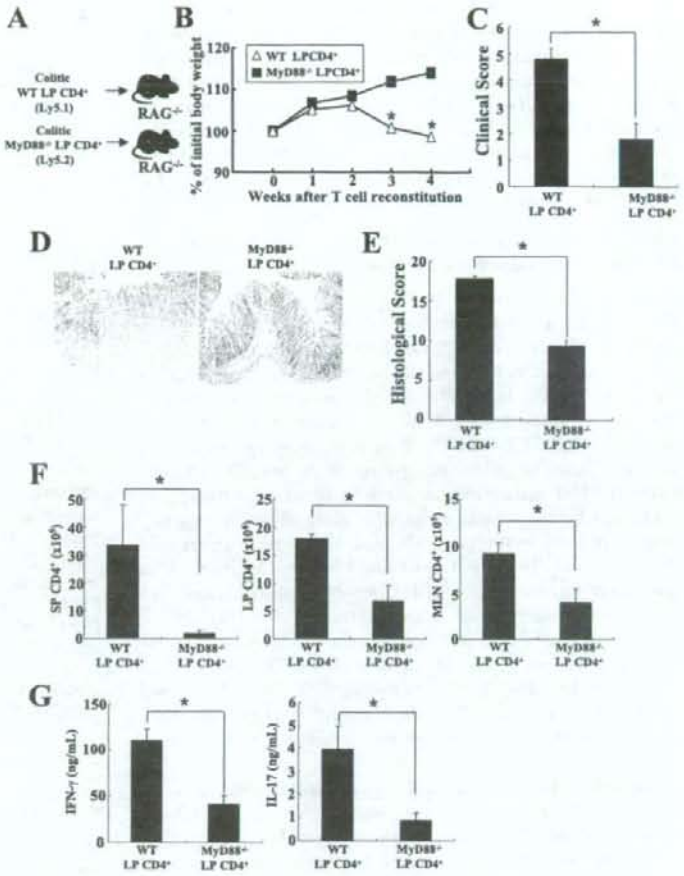

FIGURE 6. RAG-$2^{-/-}$ mice transferred with colitogenic MyD88$^{-/-}$ LP CD4$^+$ T cells develop milder colitis. *A*, RAG-$2^{-/-}$ mice were transferred with colitogenic MyD88$^{+/+}$ (WT) ($n = 6$) or MyD88$^{-/-}$ ($n = 6$) LP CD4$^+$ T cells (4×10^5 cells/mouse). *B*, Change in body weight is expressed as percent of the original weight. Data are represented as mean ± SEM of six mice in each group. *, $p < 0.05$. *C*, Clinical scores were determined at 4 wk after transfer as described in *Materials and Methods*. Data are indicated as mean ± SEM of six mice in each group. *, $p < 0.01$. *D*, Histological examination of the colon from mice transferred with colitic WT (*left*) or MyD88$^{-/-}$ (*right*) CD4$^+$ T cells at 4 wk after transfer. Original magnification, ×100. *E*, Histological scoring of mice transferred with colitic WT or MyD88$^{-/-}$CD4$^+$ T cells at 4 wk after transfer. Data are indicated as mean ± SEM of six mice in each group. *, $p < 0.05$. *F*, LP, MLN, and SP CD4$^+$ T cells were isolated from of mice transferred with colitic WT or MyD88$^{-/-}$CD4$^+$ T cells at 4 wk after transfer, and the number of CD4$^+$ cells was determined by flow cytometry. Data are indicated as mean ± SEM of six mice in each group. *, $p < 0.05$. *G*, Cytokine production by LP CD4$^+$ T cells. LP CD4$^+$ T cells were isolated at 4 wk after transfer and stimulated with anti-CD3 and -CD28 mAbs for 48 h. IFN-γ and IL-17 concentrations in culture supernatants were measured by ELISA. Data are indicated as mean ± SEM of six mice in each group. *, $p < 0.05$.

MyD88$^{-/-}$ donor cells as compared with mice transferred with MyD88$^{+/+}$ donor cells. To further address the survival of CD4$^+$ T cells, we next assessed whether regulation of Bcl-2 and Bcl-x_L expression requires the MyD88-dependent signaling pathway using a quantitative RT-PCR. As expected, the SP CD4$^+$ T cells from mice transferred with MyD88$^{-/-}$ donor cells expressed a significantly lower level of Bcl-2 and Bcl-x_L compared with those from mice transferred with MyD88$^{+/+}$ donor cells (Fig. 2*H*). We also examined the cytokine production by isolated LP CD4$^+$ T cells from recipient mice transferred with MyD88$^{+/+}$ or MyD88$^{-/-}$ donor cells along with LP CD4$^+$ T cells from healthy MyD88$^{+/+}$ or MyD88$^{-/-}$ mice. As shown in Fig. 2*I*, LP CD4$^+$ T cells from mice transferred with MyD88$^{-/-}$ donor cells produced significantly less IFN-γ and IL-17 as compared with those from mice transferred with MyD88$^{+/+}$ donor cells upon in vitro stimulation by anti-CD3/anti-CD28 mAbs. LP CD4$^+$ T cells from both healthy WT and MyD88$^{-/-}$ mice produced only a small amount of these cytokines, showing no significant difference under the same condition (Fig. 2*I*).

Vβ repertoire is almost constant regardless of WT or MyD88$^{-/-}$ donor cells

Although we found that mice transferred with MyD88$^{-/-}$ donor cells develop milder colitis compared with mice transferred with MyD88$^{+/+}$ donor cells, possibly due to the lack of a MyD88 pathway within CD4$^+$ T cells, it remained unclear whether expanded CD4$^+$ T cells in the recipient mice recognize the same antigenic epitopes of CD4$^+$ T cells. To clarify this issue, SP CD4$^+$ T cells from both groups of mice were analyzed for their TCR Vβ repertoire by flow cytometry. As shown in Fig. 3, the polyclonal dominant TCR Vβ repertoire with the dominancy of Vβ8.1/8.2 and Vβ8.3 was almost constant regardless of MyD88$^{+/+}$ or MyD88$^{-/-}$ donor cells. Only the frequency of Vβ5.1/5.2 in mice transferred with MyD88$^{-/-}$ donor cells was significantly increased as compared with that in mice transferred with WT donor cells, indicating that colitogenic CD4$^+$ T cells recognizing the same or similar Ag epitopes could develop independently from the TLR-MyD88 signaling pathway in CD4$^+$ T cells.

Expansive activity of WT donor cells predominates over that of MyD88$^{-/-}$ donor cells in in vivo competition assay

To further assess the requirement of TLR-MyD88 signaling for the expansion of CD4$^+$ donor cells, we performed in vivo competition experiments. The same number (2.5×10^5 cells/mouse) of CD4$^+$CD45RB^{high} donor cells from Ly5.1-background (Ly5.1$^+$) MyD88$^{+/+}$ and Ly5.2-background (Ly5.2$^+$) MyD88$^{-/-}$ mice were coinjected i.p. into the identical RAG-$2^{-/-}$ mice (Fig. 4*A*). As expected, recipient mice developed severe colitis at 6 wk after cotransfer (data not shown), and a significantly lower proportion of Ly5.2$^+$ MyD88$^{-/-}$ CD4$^+$ T cells was observed not only in the inflamed LP, but also in SP,

MLN, PB, and BM, as compared with the paired Ly5.1$^+$MyD88$^{+/+}$CD4$^+$ T cells (Fig. 4*B*). Furthermore, the ratio of IFN-γ-expressing cells within total MyD88$^{-/-}$ LP CD4$^+$ T cells was significantly lower compared with that in total MyD88$^{+/+}$ LP CD4$^+$ T cells (Fig. 4*C*). Consistent with the lower expression of IFN-γ in MyD88$^{-/-}$ LP CD4$^+$ T cells, expression of the activation marker CD69 on MyD88$^{-/-}$ LP or SP CD4$^+$ cells was significantly lower than on MyD88$^{+/+}$ LP or SP CD4$^+$ T cells, respectively (Fig. 4*D*).

RAG-2$^{-/-}$ mice transferred with MyD88$^{-/-}$ colitogenic LP CD4$^+$ donor cells develop milder colitis

To next assess the role of MyD88-dependent pathway in persistent colitis, we next examined colitogenic LP CD4$^+$ T cell-mediated colitis model (17), which lacks the impact of naive T cell priming, activation, and differentiation phase required in the former CD4$^+$CD45RB^{high} T cell-transferred colitis model. We first confirmed that RAG-2$^{-/-}$ mice transferred with MyD88$^{-/-}$CD4$^+$CD45RB^{high} T cells do develop colitis to a similar extent to mice transferred with MyD88$^{+/+}$CD4$^+$ CD45RB^{high} T cells at the late stage of 10 wk after transfer as confirmed by the weight curve (Fig. 5*A*), albeit the ongoing disease activity index (Fig. 5*B*) and histological assessment (Fig. 5, *C* and *D*) delayed onset and kinetics. Consistent with these findings, the recovered cell number was equivalent between mice transferred with MyD88$^{+/+}$ or MyD88$^{-/-}$ CD4$^+$CD45RB^{high} T cells (Fig. 5*E*). Furthermore, the expression of activation (CD69)/differentiation (IL-7Rα, CD44, and CD62L) on LP CD4$^+$ T cells showed no difference between two groups of mice (Fig. 5*F*), indicating that MyD88 deficiency solely contributes to the delayed kinetics of the development of colitis.

We thus isolated the LP CD4$^+$ T cells from colitic recipient mice transferred with either MyD88$^{+/+}$ or MyD88$^{-/-}$ CD4$^+$CD45RB^{high} T cells at 10 wk after transfer, to use for the subsequent memory T cell transfer. We transferred the isolated colitic LP CD4$^+$ T cells into new RAG-2$^{-/-}$ mice to focus on the persistence of colitogenic CD4$^+$ memory T cells (Fig. 6*A*). Similar with the results using CD4$^+$CD45RB^{high} T cell-mediated colitis model in Fig. 2, the recipient mice transferred with colitic MyD88$^{-/-}$ LP CD4$^+$ T cells showed milder wasting disease (Fig. 6*B*) with milder clinical signs of colitis at 4 wk after retransfer, as compared with mice transferred with colitic MyD88$^{+/+}$ LP CD4$^+$ T cells (Fig. 6*C*). Histological examination also revealed that mice transferred with MyD88$^{-/-}$ LP CD4$^+$ T cells developed milder colitis at 4 wk after retransfer as compared with mice transferred with MyD88$^{+/+}$ LP CD4$^+$ T cells (Fig. 6*D*). The difference was statistically confirmed by histological scoring of colon sections, which showed as follows: mice transferred with MyD88$^{+/+}$ LP CD4$^+$ T cells, 17.8 ± 0.86 and mice transferred with MyD88$^{-/-}$ LP CD4$^+$ T cells, 9.4 ± 1.86 ($p < 0.01$) (Fig. 6*E*). Furthermore, a significantly lower number of CD4$^+$ T cells was recovered from SP, LP, and MLN of mice transferred with MyD88$^{-/-}$ donor cells as compared with mice transferred with MyD88$^{+/+}$ donor cells (Fig. 6*F*). As shown in Fig. 6*G*, LP CD4$^+$ T cells from mice transferred with MyD88$^{-/-}$ LP donor cells produced significantly less IFN-γ and IL-17 as compared with those from mice transferred with MyD88$^{+/+}$ LP donor cells.

To further assess the expansive activity of colitic LP CD4$^+$ memory T cells, we again performed in vivo competition experiments. The same number (2.0×10^5 cells/mouse) of colitic Ly5.1$^+$MyD88$^{+/+}$ and Ly5.2$^+$MyD88$^{-/-}$ LP donor cells obtained from colitic mice transferred with Ly5.1$^+$MyD88$^{+/+}$ or

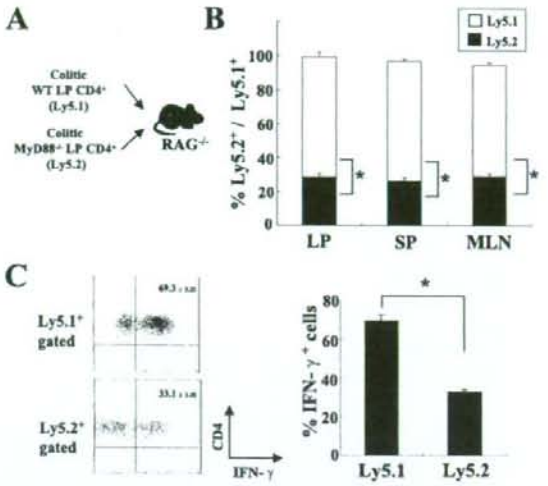

FIGURE 7. Expansion activity of colitic MyD88$^{+/+}$ LP donor cells predominates over that of MyD88$^{-/-}$ donor cells in an in vivo competition assay. *A*, The same number (2.0×10^5 cells/mouse) of colitic LP MyD88$^{+/+}$ (WT) (Ly5.1$^+$) and MyD88$^{-/-}$ (Ly5.2$^+$) CD4$^+$ T cells mice was injected i.p. into RAG-2$^{-/-}$ mice ($n = 6$). *B*, Six weeks after transfer, LP, SP, and MLN CD4$^+$ T cells were isolated from mice, and the ratio of Ly5.1$^+$ and Ly5.2$^+$ CD4$^+$ cells was determined by flow cytometry. *, $p < 0.01$. *C*, The frequencies of IFN-γ-producing cells per the total Ly5.1$^+$ or Ly5.2$^+$ cells were analyzed in the indicated subpopulations by flow cytometry. Data are represented as mean ± SEM of three independent experiments. *, $p < 0.01$.

Ly5.2$^+$MyD88$^{-/-}$ CD4$^+$CD45RB^{high} T cells at 10 wk after transfer was coinjected i.p. into identical RAG-2$^{-/-}$ mice (Fig. 7*A*). Six wk after cotransfer, a significantly lower proportion of Ly5.2$^+$ MyD88$^{-/-}$CD4$^+$ T cells was recovered from the inflamed LP, SP, and MLN, as compared with the paired Ly5.1$^+$MyD88$^{+/+}$CD4$^+$ T cells (Fig. 7*B*). Furthermore, the ratio of IFN-γ-expressing CD4$^+$ T cells within total MyD88$^{-/-}$ LP CD4$^+$ T cells was significantly decreased as compared with that within total MyD88$^{+/+}$ LP CD4$^+$ T cells (Fig. 7*C*).

MyD88 signaling contributes to the lymphopenia-driven rapid proliferation of colitogenic CD4$^+$ T cells

To finally examine the effect of MyD88 signaling on the lymphopenia-driven rapid proliferation (18) of the colitogenic CD4$^+$ memory T cells, we used the in vivo CFSE dilution method to examine cells undergoing proliferation after a short period from transfer. First, the LP CD4$^+$ T cells obtained from colitic RAG-2$^{-/-}$ mice transferred with either MyD88$^{+/+}$ or MyD88$^{-/-}$ CD4$^+$CD45RB^{high} T cells at 10 wk after transfer were labeled with CFSE and adoptively cotransferred into new RAG-2$^{-/-}$ mice. Cell divisions were determined 10 days after cotransfer by assessing the CFSE dilution (Fig. 8*A*). As depicted in Fig. 8*B*, the markedly delayed division pattern of CD4$^+$ T cells from mice transferred with MyD88$^{-/-}$ donor cells was observed as compared with that in mice transferred with MyD88$^{+/+}$ donor cells. This difference was statistically confirmed by comparing the CFSE$^+$ cells between Ly5.1$^+$ and Ly5.2$^+$ cells (Fig. 8*C*), indicating that the MyD88-dependent signaling pathway in T cells promotes the rapid proliferation of colitogenic CD4$^+$ memory T cells in a lymphopenic condition.

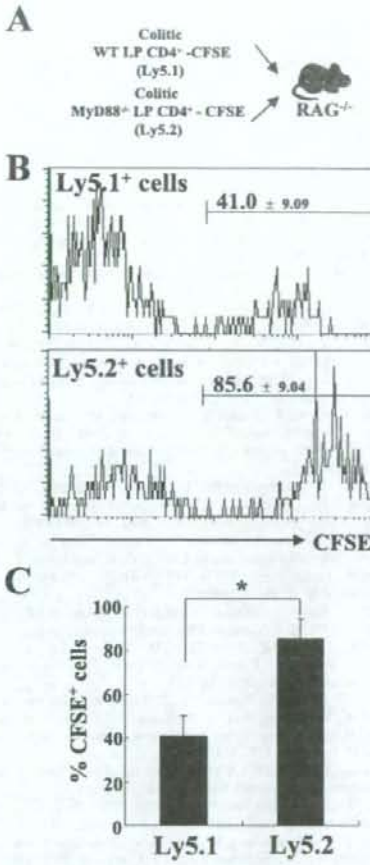

FIGURE 8. MyD88 pathway contributes to the lymphopenia-driven rapid proliferation of colitogenic $CD4^+$ T cells. *A*, The same number (2.0×10^6 cells/mouse) of CFSE-labeled colitic LP $MyD88^{+/+}$ (WT) ($Ly5.1^+$) and $MyD88^{-/-}$ ($Ly5.2^+$) $CD4^+$ T cells were coinjected i.p. into new RAG-$2^{-/-}$ mice ($n = 6$). *B*, The donor cells in the host spleen were analyzed 10 days after transfer by staining CD4, Ly5.1, and Ly5.2. Histograms show CFSE profiles of the two donor cell types in the host spleen. Data are representative of five independent experiments. *C*, Percentages of positive CFSE staining per total $Ly5.1^+$ or $Ly5.2^+$ cells were analyzed in the indicated subpopulations by flow cytometry. Data are represented as mean ± SEM of three independent experiments. *, $p < 0.05$.

Discussion

In the present study, we demonstrated that the MyD88-dependent signaling pathway in T cells directly modulates the proliferation and survival of TLRs/MyD88-expressing colitogenic $CD4^+$ T cells during the development and persistence of colitis. So far, it has been believed that T cell activation and expansion is induced and maintained by TCR signaling through the interaction with Ag-loading DCs that are primarily activated by PAMP/TLR-induced maturation (21). However, this study provides a new pathway by which the MyD88-dependent signaling pathway within $CD4^+$ T cells may directly play a pivotal role in the acquired immune components of chronic colitis by enhancing PAMP-specific immune responses collaborating with Ag-specific TCR signaling and homeostatic cytokines, such as IL-7 and IL-15 (18, 22–24).

How do commensal bacteria-derived PAMPs contribute to the maintenance of colitogenic $CD4^+$ T cells during the perpetuation of colitis? In other words, from where do colitogenic $CD4^+$ T cells receive proliferative and/or survival signals to sustain chronic colitis? First, it is well-known that commensal bacteria are essentially required for the development and the persistence of colitis, because 1) almost all models of T cell-mediated colitis do not develop colitis under the germfree condition (4–6), and 2) several groups elegantly demonstrated the requirement of specific Ags for the development and persistence of colitis by showing that colitis is induced and sustained by administration of OVA peptide-expressing *Escherichia coli* into OVA-specific TCR-transgenic mice in an Ag-specific manner (25, 26). These results indicated that TCR signaling through Ags, especially Ags derived from commensals, are needed for the development and persistence of colitis. Second, in addition to Ags derived from commensal bacteria, we here showed that the MyD88-dependent signaling pathway directly bolsters up the proliferation and survival of colitogenic $CD4^+$ T cells. However, it is of note that RAG-$2^{-/-}$ mice transferred with $MyD88^{-/-}$ $CD4^+CD45RB^{high}$ T cells did develop colitis with $CD4^+$ T cell infiltration in the inflamed mucosa albeit the onset was delayed as compared with the control, indicating that the direct MyD88-dependent signaling pathway in colitogenic $CD4^+$ T cells may act as a costimulator to tune the essential TCR signaling for the maintenance of these cells. However, at the molecular level, it still remains unknown how the identical $CD4^+$ T cells coordinate TCR and TLR signaling initiated from the commensal bacteria for activation, proliferation, and survival. Further studies will be required to address this important issue.

So far, most studies regarding TLRs have focused on cells of the innate immune system, such as DCs, macrophages, and epithelial cells, and now it is recognized that members of TLRs play an essential role in the innate immune recognition allowing the detection of commensal bacteria, followed by the second activation of T cells (9–11). However, recent works showed that conventional TCR $\alpha\beta^+CD4^+$ T cells also express TLRs (12), suggesting that PAMPs may directly modulate the function of $CD4^+$ T cells. Importantly, Gelman et al. (27) recently reported that TLR signaling in primary $CD4^+$ T cells directly enhances proliferation through MyD88 and PI3K-dependent pathway, in response to a T cell-dependent Ag. Thus, the present study may add the identification of the role of TLR signaling in the activation/function of the pathogenic memory $CD4^+$ T cells. Although we showed that the MyD88-dependent signaling pathway positively reinforces the proliferation and survival of colitogenic $CD4^+$ T cells in colitic mice, it has been previously reported that TLR-4 is predominantly expressed on regulatory $CD4^+CD25^+$ T cells rather than $CD4^+CD45RB^{high}$ naive cells, and TLR-4-specific signaling by LPS increases the regulatory $CD4^+CD25^+$ T cell activity, resulting in suppression of inflammatory responses in vivo (16). We slightly, but substantially, detected TLR-4 mRNA as well as other TLRs in colitic LP $CD4^+$ T cells, thus it is interesting to know how the stimulatory and inhibitory TLR-signaling pathway in T cells orchestrates the complicated immune responses in chronic colitis.

Such characteristics of TLR/MyD88-expressing colitogenic $CD4^+$ T cells raise another important question of whether the colitogenic $CD4^+CD44^{high}CD62L^-$IL-$7R\alpha^{high}$ T cells (Fig. 2) can be defined as effector-memory T cells rather than just effector T cells under the persistent presence of commensal Ags and/or self Ags, because it is accepted that memory T cells are generated after Ag clearance for the first time, but not under persistent presence of Ags, shown in models of chronic viral infections to $CD8^+$ T cells, using lymphocytic choriomeningitis virus or influenza A virus infections (28). Because the candidate Ags for colitogenic $CD4^+$ T cells are thought to be derived

from the intestinal bacterial Ags that are never eliminated from the body, it is doubtful whether colitogenic $CD4^+$ memory T cells can be generated under such a situation. However, as recent studies have suggested that persistent presence of Ags is rather required for the long-term maintenance of $CD4^+$ memory T cells, it is possible that the nature of $CD4^+$ memory T cells is quite different from that of $CD8^+$ memory T cells (29, 30). Thus, the present results may support another idea that the persistent presence of both commensal bacteria-derived PAMPs and specific Ags is required for the maintenance of long-term colitogenic $CD4^+$ memory T cells, and the subsequent progressive, disabling disease course.

It is also possible that nonpathogenic commensals stimulate TLR signaling of colitogenic $CD4^+$ memory T cells to sustain the disease without providing specific Ags for such cells. In other words, it should be verified whether specific Ags or PAMPs from the commensal bacteria are essential for the priming or memory phase. Consistently, the current study also provides an explanation of why a common recurrence of IBD is observed during complication of microbial infection, such as acute *Salmonella enterocolitis*, which may possibly supply large amounts of "bystander" PAMPs (31).

Finally, an important point should also be discussed: whether the present experimental design solely assesses the role of direct TLR signaling in various stages of $CD4^+$ T cells during the development of chronic colitis, because MyD88 is also involved in signaling downstream of endogenous cytokines, IL-1 and IL-18, in addition to TLR signaling (13, 14). Further studies will be required to address this issue by assessing which TLR is the most important for the stimulation of colitogenic $CD4^+$ T cells, followed by in vivo experiment using the corresponding TLR^{mut} mice.

In summary, we here demonstrate that the MyD88-dependent pathway that mediates downstream signals of TLRs is crucially involved in the proliferative and survival responses of colitogenic $CD4^+$ T cells, which is required for the perpetuation of chronic colitis. Thus, in addition to the specific commensal Ags, homeostatic cytokines, and costimulatory molecules, therapeutic approaches targeting PAMPs may be feasible in the treatment of IBD.

Disclosures

The authors have no financial conflict of interest.

References

1. Podolsky, D. K. 2002. Inflammatory bowel disease. *N. Engl. J. Med.* 347: 417–429.
2. Baumgart, D. C., and S. R. Carding. 2007. Inflammatory bowel disease: cause and immunobiology. *Lancet* 369: 1627–1640.
3. Strober, W., I. J. Fuss, and R. S. Blumberg. 2002. The immunology of mucosal models of inflammation. *Annu. Rev. Immunol.* 20: 495–549.
4. Seksik, P., H. Sokol, P. Lepage, N. Vasquez, C. Manichanh, I. Mangin, P. Pochart, J. Dore, and P. Marteau. 2006. Review article: the role of bacteria in onset and perpetuation of inflammatory bowel disease. *Aliment. Pharmacol. Ther.* 24(Suppl. 3): 11–18.
5. Sartor, R. B. 2006. Mechanisms of disease: pathogenesis of Crohn's disease and ulcerative colitis. *Nat. Clin. Pract. Gastroenterol. Hepatol.* 3: 390–407.
6. Izcue, A., J. L. Coombes, and F. Powrie. 2006. Regulatory T cells suppress systemic and mucosal immune activation to control intestinal inflammation. *Immunol. Rev.* 212: 256–271.
7. Bamias, G., M. R. Nyce, S. A. De La Rue, and F. Cominelli. 2005. New concepts in the pathophysiology of inflammatory bowel disease. *Ann. Intern. Med.* 143: 895–904.
8. Hibi, T., and H. Ogata. 2006. Novel pathophysiological concepts of inflammatory bowel disease. *J. Gastroenterol.* 41: 10–16.
9. Akira, S., S. Uematsu, and O. Takeuchi. 2006. Pathogen recognition and innate immunity. *Cell* 124: 783–801.
10. Rakoff-Nahoum, S., and R. Medzhitov. 2006. Role of the innate immune system and host-commensal mutualism. *Curr. Top. Microbiol. Immunol.* 308: 1–18.
11. Schnare, M., G. M. Barton, A. C. Holt, K. Takeda, S. Akira, and R. Medzhitov. 2001. Toll-like receptors control activation of adaptive immune responses. *Nat. Immunol.* 2: 947–950.
12. Kabelitz, D. 2007. Expression and function of Toll-like receptors in T lymphocytes. *Curr. Opin. Immunol.* 19: 39–45.
13. Adachi, O., T. Kawai, K. Takeda, M. Matsumoto, H. Tsutsui, M. Sakagami, K. Nakanishi, and S. Akira. 1998. Targeted disruption of the *MyD88* gene results in loss of IL-1- and IL-18-mediated function. *Immunity* 9: 143–150.
14. Medzhitov, R., P. Preston-Hurlburt, E. Kopp, A. Stadlen, C. Chen, S. Ghosh, and C. A. Janeway, Jr. 1998. MyD88 is an adaptor protein in the hToll/IL-1 receptor family signaling pathways. *Moll. Cell* 2: 50–53.
15. Totsuka, T., T. Kanai, R. Iiyama, K. Uraushihara, M. Yamazaki, R. Okamoto, T. Hibi, K. Tezuka, M. Azuma, H. Akiba, et al. 2003. Ameliorating effect of anti-ICOS monoclonal antibody in a murine model of chronic colitis. *Gastroenterology* 124: 410–421.
16. Caramalho, I., T. Lopes-Carvalho, D. Ostler, S. Zelenay, M. Haury, and J. Demengeot. 2003. Regulatory T cells selectively express toll-like receptors and are activated by lipopolysaccharide. *J. Exp. Med.* 197: 403–411.
17. Kanai, T., K. Tanimoto, Y. Nemoto, R. Fujii, S. Makita, T. Totsuka, and M. Watanabe. 2006. Naturally arising $CD4^+CD25^+$ regulatory T cells suppress the expansion of colitogenic $CD4^+CD44^{high}CD62L^-$ effector memory T cells. *Am. J. Physiol.* 290: G1051–G1058.
18. Totsuka, T., T. Kanai, Y. Nemoto, S. Makita, R. Okamoto, K. Tsuchiya, and M. Watanabe. 2007. IL-7 is essential for the development and the persistence of chronic colitis. *J. Immunol.* 178: 4737–4748.
19. Surh, C. D., O. Boyman, J. F. Purton, and J. Sprent. 2006. Homeostasis of memory T cells. *Immunol. Rev.* 211: 154–163.
20. Makita, S., T. Kanai, Y. Nemoto, T. Totsuka, R. Okamoto, K. Tsuchiya, M. Yamamoto, H. Kiyono, and M. Watanabe. 2007. Intestinal lamina propria retaining $CD4^+CD25^+$ regulatory T cells is a suppressive site of intestinal inflammation. *J. Immunol.* 178: 4937–4946.
21. Kaisho, T., and S. Akira. 2001. Dendritic-cell function in Toll-like receptor- and MyD88-knockout mice. *Trends Immunol.* 22: 78–83.
22. Bradley, L. M., L. Haynes, and S. L. Swain. 2005. IL-7: maintaining T-cell memory and achieving homeostasis. *Trends Immunol.* 26: 172–176.
23. Seddon, B., P. Tomlinson, and R. Zamoyska. 2003. Interleukin 7 and T cell receptor signals regulate homeostasis of CD4 memory cells. *Nat. Immunol.* 4: 680–686.
24. Picker, L. J., E. F. Reed-Inderbitzin, S. I. Hagen, J. B. Edgar, S. G. Hansen, A. Legasse, S. Planer, M. Piatak, Jr., J. D. Lifson, V. C. Maino, et al. 2006. IL-15 induces CD4 effector memory T cell production and tissue emigration in nonhuman primates. *J. Clin. Invest.* 116: 1514–1524.
25. Iqbal, N., J. R. Oliver, F. H. Wagner, A. S. Lazenby, C. O. Elson, and C. T. Weaver. 2002. T helper 1 and T helper 2 cells are pathogenic in an antigen-specific model of colitis. *J. Exp. Med.* 195: 71–84.
26. Yoshida, M., T. Watanabe, T. Usui, Y. Matsunaga, Y. Shirai, M. Yamori, T. Itoh, S. Habu, T. Chiba, T. Kita, and Y. Wakatsuki. 2001. T cells monospecific to ovalbumin produced by *Escherichia coli* can induce colitis upon transfer to BALB/c and SCID mice. *Int. Immunol.* 13: 1561–1570.
27. Gelman, A. E., D. F. LaRosa, J. Zhang, P. T. Walsh, Y. Choi, J. O. Sunyer, and L. A. Turka. 2006. The adaptor molecule MyD88 activates PI-3 kinase signaling in $CD4^+$ T cells and enables CpG oligodeoxynucleotide-mediated costimulation. *Immunity* 25: 783–793.
28. Klenerman, P., and A. Hill. 2005. T cells and viral persistence: lessons from diverse infections. *Nat. Immunol.* 6: 873–879.
29. Robertson, J. M., M. MacLeod, V. S. Marsden, J. W. Kappler, and P. Marrack. 2006. Not all $CD4^+$ memory T cells are long lived. *Immunol. Rev.* 211: 49–57.
30. Zaph, C., J. Uzonna, S. M. Beverley, and P. Scott. 2004. Central memory T cells mediate long-term immunity to Leishmania major in the absence of persistent parasites. *Nat. Med.* 10: 1104–1110.
31. Stallmach, A., and O. Carstens. 2002. Role of infections in the manifestation or reactivation of inflammatory bowel diseases. *Inflamm. Bowel. Dis.* 8: 213–218.

Involvement of Smad3 phosphoisoform-mediated signaling in the development of colonic cancer in IL-10-deficient mice

DAISAKU HACHIMINE[1], KAZUSHIGE UCHIDA[1], MASANORI ASADA[2], AKIYOSHI NISHIO[2], SEIJI KAWAMATA[1], GO SEKIMOTO[1], MIKI MURATA[1], HIDEO YAMAGATA[1], KATSUNORI YOSHIDA[1], SHIGEO MORI[1], YOSHIYA TAHASHI[1], KOICHI MATSUZAKI[1] and KAZUICHI OKAZAKI[1]

[1]Third Department of Internal Medicine, Kansai Medical University, Moriguchi, Osaka;
[2]Department of Gastroenterology, Graduate School of Medicine, Kyoto University, Kyoto, Japan

Received February 7, 2008; Accepted March 19, 2008

Abstract. Chronic inflammation predisposes to cancer. Transforming growth factor (TGF)-ß, a multifunctional protein, suppresses the growth of normal colonic epithelial cells, whereas it stimulates the proliferation of cancer cells. Interleukin (IL)-10-deficient mice, which develop colitis and colorectal cancer, show an increased level of plasma TGF-ß. Although TGF-ß may be a key molecule in the development of colon cancer arising from chronic colitis in IL-10-deficient mice, the role of TGF-ß still remains unclear. TGF-ß activates not only TGF-ß type I receptor (TßRI) but also c-Jun N-terminal kinase (JNK), which converts the mediator Smad3 into two distinctive phosphoisoforms: C-terminally phosphorylated Smad3 (pSmad3C) and linker-phosphorylated Smad3 (pSmad3L). We studied C57BL/6-IL-10-deficient mice (n=18) at 4 to 32 weeks of age. We investigated histology, and pSmad2/3L, pSmad2/3C, and p53 by immunohistochemistry. pSmad3L staining was detected in the cancer cells in all 10 mice with colonic cancer and in the epithelial cells in 7 of 12 mice with colonic dysplasia, but not in the normal or colitic mice. pSmad3c was detected without any significant difference between stages. p53 was weakly stained in a few cancer cells in 5 out of 10 mice. Smad3L signaling plays an important role in the carcinogenesis of chronic colitis in IL-10-deficient mice.

Introduction

In 1925, Crohn and Rosenberg documented a case of rectal carcinoma complicating ulcerative colitis (UC) and postulated that the lesion developed as a late manifestation of the disease (1), and many subsequent epidemiological studies have confirmed this increased risk (as high as 34%) after 25 years of disease (2). In contrast to sporadic colorectal cancers, which develop through the 'adenoma-carcinoma sequence', inflammatory bowel disease (IBD)-associated carcinomas develops through the 'dysplasia sequence'. Although cancers from UC as well as sporadic colorectal carcinoma are hypothesized to arise from a multistep process, the precise mechanism is still unknown.

Interleukin (IL)-10-deficient mice under specific-pathogen free conditions spontaneously develop chronic enterocolitis, a condition phenotypically similar to chronic IBD in humans (3). An increase in the incidence rate of colorectal carcinoma has been observed in conjunction with elevated plasma transforming growth factor (TGF)-ß1 levels at 10 to 31 weeks of age (4), which suggests that TGF-ß may be a key molecule in the development of colon cancer arising from chronic colitis in IL-10-deficient mice. Therefore, this murine IBD model may provide excellent insights into the pathogenetic mechanism of chronic colitis-associated carcinoma.

TGF-ß is a multifunctional protein that regulates a complex array of cellular processes, including proliferation, differentiation, motility, and death in a cell-specific manner (5). TGF-ß can inhibit colonic epithelial cell growth, acting as a tumor suppressor (6) and also plays a major role in the negative regulation of immune cell functions, particularly in the gut (7). Loss of TGF-ß (8) or unresponsiveness to TGF-ß1 (9) in the colonic epithelium has been associated with the development or progression of inflammation in the colon. However, increased TGF-ß activity may be involved in tumor development rather than tumor suppression in IL-10-deficient mice (5). The role of TGF-ß in tumor development thus seems to be dual, and dependent on the stage of the tumor. These multiple functions are thought to result from different intracellular signaling pathways. Recent evidence suggests that TGF-ß is also a key regulator of epithelial-to-mesenchymal transition (EMT) in cell phenotypes (10). EMT not only underlies epithelial degeneration and fibrogenesis in chronic degenerative disorders, but also endows dedifferentiated malignant epithelial cells with mesenchymal, migratory, and proteolytic properties that are required for local tumor invasiveness (11). Inhibition of the pro-inflammatory cytokine IL-1ß at initiation of EMT has been

Correspondence to: Dr Kazuichi Okazaki, Third Department of Internal Medicine, Kansai Medical University, 10-15 Fumizono-cho, Moriguchi, Osaka, 570-8506, Japan
E-mail: okazaki@hirakata.kmu.ac.jp

Key words: Smad3, colonic cancer, interleukin-10

found to attenuate fibrogenesis (12), suggesting a causative link between chronic inflammation and EMT. The main downstream signaling pathway for TGF-ß involves the Smad proteins (13). Although several studies of EMT have suggested that the process involves Smad-independent pathways (14), recent studies using Smad3 knockout mice have indicated that signaling through the Smad3-dependent pathway is required for injury-dependent multistage transition of an epithelial cell to a mesenchymal phenotype (15). Therefore, we focused on Smad3 signaling (16,17), and on the different roles of Smad3 phosphoisoform-mediated signaling in epithelial cells and mesenchymal cells, reported recently (18). Thus, TGF-ß activates not only TGF-ß type I receptor (TßRI) but also c-Jun N-terminal kinase (JNK), converting Smad3 into two distinct phosphoisoforms: C-terminally phosphorylated Smad3 (pSmad3C) and linker-phosphorylated Smad3 (pSmad3L). The TßRI/pSmad3C pathway inhibits growth of epithelial cells, while JNK/pSmad3L-mediated signaling promotes ECM deposition by activated mesenchymal cells such as hepatic stellate cells (HSCs) (5). However, it is unclear how Smad3 signaling is involved in the development of colon cancer during long-standing chronic colitis.

In the present study, according to these phosphorylation-defined activities, we studied whether Smad3 phosphoisoforms govern progression from chronic colitis to colonic cancer in an IL-10-deficient mouse model.

Materials and methods

Animals. C57BL/6-IL-10-deficient mice (aged 4-32 weeks) were purchased from The Jackson Laboratory (Bar Harbor, ME). The animals were housed under specific-pathogen free (SPF) conditions and fed autoclaved food and sterile water in the animal facility of the Graduate School of Medicine, Kyoto University. Of these, the IL-10-deficient mice were transferred from SPF to conventional housing conditions at six weeks of age as they spontaneously develop colitis under conventional housing conditions by eight weeks of age. All animal experiments were performed in accordance with our institutional guidelines.

Histology. The entire large intestines were examined in 18 IL-10-deficient mice between 4 and 32 weeks of age. The large intestines were fixed in 4.5% buffered formaldehyde before embedding in paraffin blocks. For histological analysis, 5-μm sections were cut and stained with hematoxylin and eosin (H&E). The principal histologic distinction was between dysplasia and colorectal carcinoma according to Japanese criteria. Histologic slides involving diagnoses of normal, dysplasia and adenocarcinoma were reviewed independently by two pathologists specialising in gastrointestinal neoplasia.

Domain-specific Abs against the phosphorylated Smad3. Polyclonal anti-phospho-Smad3 antibodies [anti-pSmad3L ($Ser^{207/212}$) and anti-pSmad3C ($Ser^{423/425}$)] were raised against the phosphorylated linker regions and COOH-terminal regions of Smad3 by immunization of rabbits with synthetic peptides. The relevant antisera were affinity purified with the phosphorylated peptides as described previously (16).

Table 1. Serial analysis of intestines in IL-10-deficient mice.

Age (weeks)	n	Colitis	Dysplasia	Cancer
4	3	0	0	0
7	1	1	0	0
8	2	2	2	0
12	2	2	2	1
16	2	2	2	2
24	2	2	2	2
28	4	4	4	4
32	2	2	2	2

Immunohistochemistry. Immunohistochemical staining was performed on formalin-fixed, paraffin-embedded tissue sections. The sections were deparaffinized in xylene, and rehydrated in graded alcohols. Antigen retrieval was done by microwave irradiation in 0.01 M sodium citrate buffer (pH 6.0) for 15 min. After cooling, the endogenous peroxidase activity was blocked by incubation in 3% H_2O_2 in methanol for 10 min. After rinsing with TBS containing 0.1% Tween-20 (TBST), non-specific antigens were blocked by preincubation with 1% bovine serum albumin (Nakarai, Kyoto, Japan). The sections were incubated overnight with the following primary antibodies: anti-mouse p53 (1.0 μg/ml, Abcam, Cambridge, UK), anti-pSmad3L (1.0 μg/ml) and anti-pSmad3C (1.0 μg/ml). After rinsing with TBST, the sections were incubated with peroxidase-labeled polymer conjugated to goat anti-rabbit immunoglobulin for 1 h at room temperature. The peroxidase activity was visualized with 3,3'-diaminobenzidine (Vector Laboratories, Burlingame, CA) counterstained with Mayer's hematoxylin (Merck, Darmstadt, Germany), and mounted under coverslips. The evaluation of immunoreactivity was performed by microscopy (Olympus BX 50, Tokyo, Japan). Immunohistochemistry was scored by pathologists in double-blind fashion according to staining proportions as follows: 0, no staining seen; 1, staining seen in 5-30% of cells; 2, staining seen in >30% of cells.

Statistical analysis. Statistical evaluation was done using the nonparametrical Mann-Whitney U ranking test. Values were based on two-tailed statistical analysis.

Results

Development of colorectal dysplasia and carcinomas in IL-10-deficient mice. We confirmed a previous report that IL-10-deficient mice develop colitis after 7 weeks. We found that mice developed dysplasia or cancer after 8 to 12 weeks, respectively (Table I; Fig. 1). We observed no metastasis in the mesenteric lymph nodes or liver in any mice. We also observed that the small intestine was not affected.

Smad3 phosphorylation of COOH-terminals and linker regions. Immunohistochemical analysisis was performed on mice from each stage to detect Smad3 phosporylation. pSmad3C was detected without significant difference between

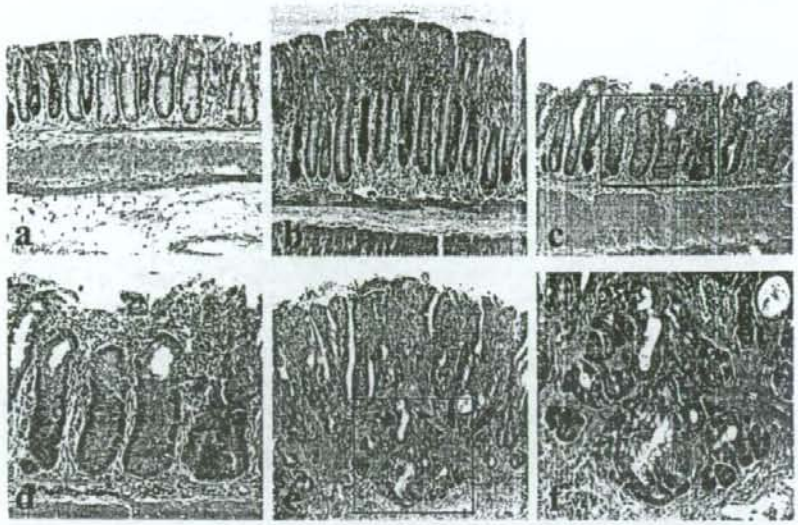

Figure 1. Histopathological findings of the colorectum in IL-10-deficient mice using hematoxylin and eosin staining (H&E). Normal colonic mucosa (a, x40). IL-10-deficient mice developed colitis (b, x40) after 7 weeks. Dysplasia (c, x40; d, x200) and cancer (e, x40; f, x200) were found after 8-12 weeks.

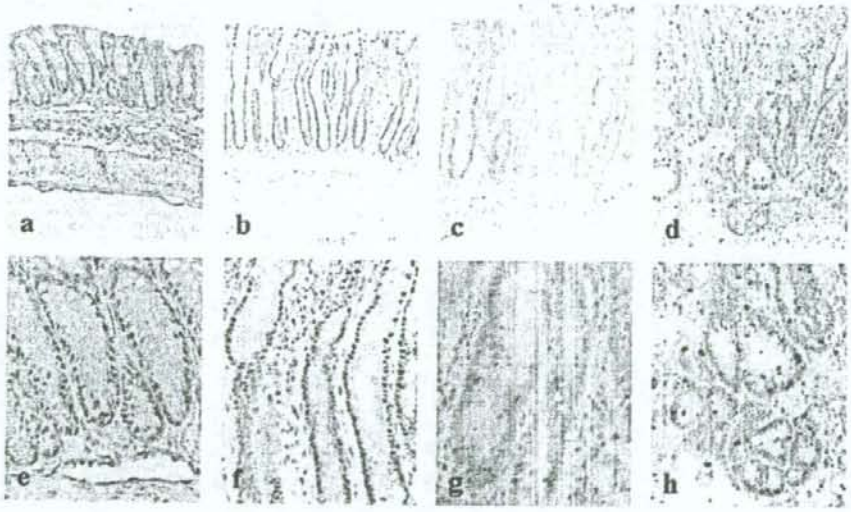

Figure 2. Immunohistochemical findings of the colorectum in IL-10-deficient mice using anti-pSamd3C antibody. pSmad3C was detected without significant difference between stages. Normal mucosa (a, x40; e, x200); colitis (b, x40; f, x200); dysplasia (c, x40; g, x200); cancer (d, x40; h, x200).

stages (Figs. 2 and 5). On the other hand, pSmad3L detection levels gradually increased from dysplasia to adenocarcinoma (Figs. 3 and 5). pSmad3L was expressed in dysplasia and cancer cells, but not in inflamed mucosa cells, even in the mice with cancer.

p53 expression in colorectal cancers. To determine p53 expression, all mice were subjected to immunohistochemical analysis using rabbit anti-mouse p53 polyclonal antibody. p53 was detected only in the mice with colonic cancer (Figs. 4 and 5). Dysplasia of the colorectal epithelium was not stained with anti-p53 antibody (Figs. 4 and 5). In 5 out of the 10 mice with cancer, the cancer cells were stained, however very few cells were p53 positive and even so stained weakly (Figs. 4 and 5).

Discussion

Colon cancer in patients with ulcerative colitis is thought to be associated with long-standing tissue injury and chronic inflammation (19). The relationship between chronic inflammation and cancer dates back to Virchow, who, in

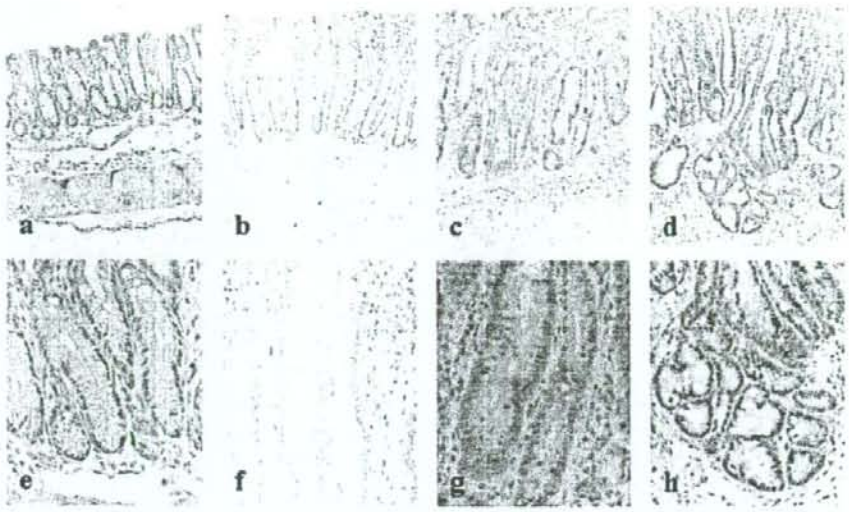

Figure 3. Immunohistochemical findings of the colorectum in IL-10-deficient mice using anti-pSamd3L antibody. pSmad3L detection levels gradually increased from dysplasia to adenocarcinoma. Normal mucosa (a, x40; e, x200); colitis (b, x40; f, x200); dysplasia (c, x40; g, x200); cancer (d, x40; h, x200).

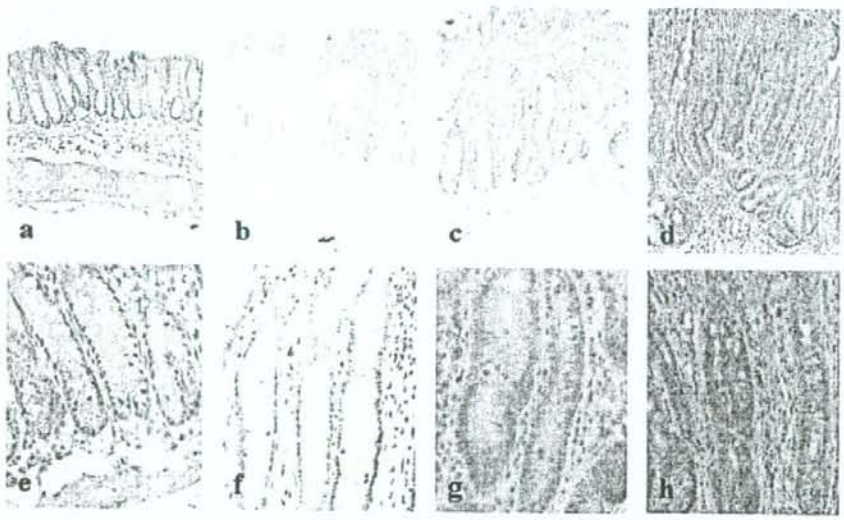

Figure 4. Immunohistochemical findings of the colorectum in IL-10 deficient mice using anti-p53 antibody. In 5 out of 10 mice with cancer, a few cancer cells were stained weakly. Normal (a, x40; e, x200); colitis (b, x40; f, x200); dysplasia (c, x40; g, x200); cancer (d, x40; h, x200).

1863, hypothesized that the origin of cancer was at sites of chronic inflammation (20). Although the relation between chronic inflammation and cancer has been well established in general, the molecular mechanisms involved in the process remain unclear. Certainly, chronic inflammation leads to increased oxidative stress. Leukocytes and other phagocytic cells generate reactive oxygen and nitrogen species, which, in turn, can damage proliferating epithelial cells. Also, chronic inflammation appears to promote the apoptosis of normal epithelial cells which can lead to a compensatory proliferative response by the remaining tissue.

Our present study confirmed that IL-10-deficient mice, spontaneously develop colonic dysplasia and cancer at a high rate following chronic colitis (4). In IL-10-deficient mice, it has been shown that serum levels of TGF-ß1 significantly increase in mice with dysplasia and cancer, compared to those without tumors (4). This led us to a hypothesize that genetic alterations in other members of the TGF-ß receptor signal transduction pathway are involved in the development of colon cancer in long-standing colitis. TGF-ß, which can potently inhibit epithelial cell growth to act as a tumor suppressor (10), is also a key regulator of epithelial-to-

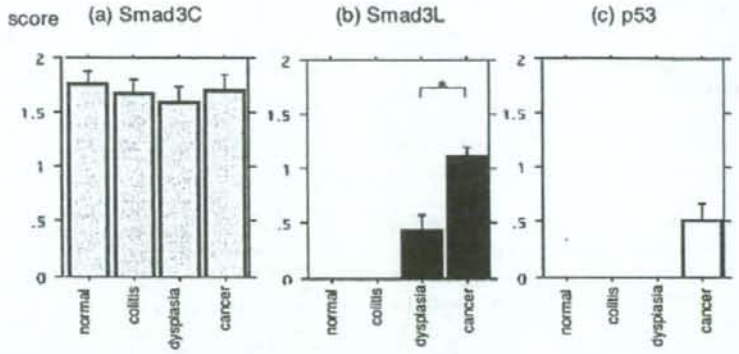

Figure 5. Immunohistochemical scores of Smad3C, 3L and p53. Immunohistochemistry was scored by pathologists in double-blind fashion according to staining proportions as follows: 0, no staining seen; 1, staining seen in 5 to 30% of cells; 2, staining seen in >30% of cells. pSmad3L detection levels increased significantly from colitis to dysplasia (0.417±0.513) to adenocarcinoma (1.100±0.316) ($p<0.05$). In normal and inflamed mucosa, even in cancerous mice, pSmad3L was not detected. Cancer cells were also stained with p53, however very few cells were positive and even so stained weakly (0.500±0.527). pSmad3C was detected without any significant difference between stages. Scores of pSmad2C staining in normal mucosa, colitis, dysplasia, and cancer were: 1.750±0.452, 1.667±0.492, 1.583±0.515, and 1.700±0.483, respectively.

mesenchymal transition (EMT) in cell phenotypes. EMT may be related to the loss of tumor responsiveness on the growth inhibitory effect of TGF-ß and at the same time to the TGF-ß-induced angiogenesis, and local and systemic immunosuppression. During carcinogenesis, tumors show EMT, thereby becoming insensitive to TGF-ß-mediated growth inhibition while showing increased tumor invasion and metastasis (10,21).

TGF-ß signaling is initiated when this ligand induces the formation of a heteromeric complex composed of TGF-ß receptor type I (TßRI) and type II (TßRII). This allows TßRII to phosphorylate TßRI, which then transmits the signal through phosphorylation of receptor-regulated Smads (R-Smads) such as Smad2 and Smad3 (22). R-Smads are directly phosphorylated at COOH-terminal SXS regions by TßRI and then undergo formation of heteromeric complexes with Smad4 (23). Activated Smad complexes are then translocated into the nucleus, where they regulate the expression of target genes both by direct DNA binding and through interaction with other transcription factors, co-activators, and co-repressors (24). Smads contain two highly conserved domains, the Mad homology 1 (MH1) and 2 (MH2) domains, which are connected by interposed linker regions (25). Although the MH1 domains can interact with DNA, the MH2 domains are endowed with transcriptional activation properties (23). In human colorectal cancer, somatic mutation of the Smad4 (18q21) or Smad2 gene (18q21) has been detected in the MH2 domain, but mutations of Smad3 (15q21), Smad6 (15q21), and Smad7 (18q21) genes have not been detected so far (26). On the other hand, Smad3-deficient mice develop colorectal carcinoma (27). Although several studies of EMT have suggested that the process involves Smad-independent pathways (23), there is evidence from Smad3-deficient mice that signaling through the Smad3-dependent pathway is required for injury-dependent multistage transition of an epithelial cell to a mesenchymal phenotype (15). As a consequence, we have focused on Smad3 signaling (16,17) and successfully developed polyclonal antibodies, which specifically recognize the phosphorylated linker regions and phosphorylated COOH-terminal SXS regions of Smad3 (17). Using these antibodies, we recently reported that Smad3 phosphorylated at linker regions or COOH-terminal regions existed as separate molecules with different functions and transmitted distinct signals (16-18). We also previously reported that as neoplasia progresses from normal colorectal epithelium through adenoma to invasive adenocarcinoma with distant metastasis, nuclear pSmad3L gradually increases while pSmad3C decreases (28). The TßRI/Smad pathway is widely represented in most cell types and tissues studied to date, and additional pathways are activated following cell stimulation by TGF-ß in specific contexts. The most prominent pathways are mediated by the mitogen activated protein kinase (MAPK) family, which consists of the extracellular signal-regulated protein kinase pathways c-Jun NH2-terminal kinase (JNK) and p38 pathways (29). TGF-ß induces activation of MAPK pathways through the upstream mediators Ras, RhoA, PP2A, and TGF-ß-activated kinase I (17). Thus, TGF-ß activates not only TßRI but also JNK, which converts Smad3 into two distinctive phosphoisoforms: pSmad3C and pSmad3L (5). Therefore, during sporadic human colorectal carcinogenesis, the shift from TßRI/pSmad3C-mediated to JNK/pSmad3L-mediated signaling is a major mechanism orchestrating a complex transition of TGF-ß signaling (5).

In the present animal study, we observed a significant increase in pSmad3L as neoplasia progressed from normal colorectal epithelium through dysplasia. Our study showed that, unlike human sporadic colon cancer, there were no changes in the phosphorylation of pSmad3C in the murine model. Moreover, no mice showed deep invasion and metastasis of cancer, which suggested that the malignant potential might be low in IL-10-deficient colitis.

The p53 mutation is known as the most common cancer-related genetic change (30). The overexpression of p53 occurs frequently in ulcerative colitis-associated colorectal carcinoma regardless of stage and pathological characteristics (31). In our results, p53 could only be detected in

some cancerous cells, and positive staining was weak. These findings, together with previous reports suggest that *p53* mutations are unlikely to be involved in the malignant transformation of epithelial cells in mice (4). Also, inactivation of *p53* may occur in the late stages of colorectal cancers developing in IL-10-deficient mice, thus being present in only a small number of tumor cells and barely detectable by the methods used in our study.

In conclusion, the phosphorylation of Smad3L may play an important role in the carcinogenesis of colorectal cancer associated with chronic colitis in IL-10-deficient mice. Further studies in human ulcerative colitis are necessary for the clarification of colitic cancer.

Acknowledgements

This study was partly supported by Grants-in-Aid for scientific program (C) from the Ministry of Science and Culture of Japan (18590755), and by Grants-in-Aid from the Health, Labor and Welfare Ministry of Japan.

References

1. Crohn BB and Rosenberg H: The sigmoidscopic picture of chronic ulcerative colitis (non-specific). Am J Med Sci 170: 220-228, 1925.
2. Kewenter J, Ahlman H and Hulten L: Cancer risk in extensive ulcerative colitis. Ann Surg 188: 824-828, 1978.
3. Reninick DM, Fort MM and Davidson NJ: Studies with IL-10-/- mice; an overview. J Leukoc Biol 61: 389-396, 1997.
4. Strulan S, Oberhuber G, Beinhauer BG, Tichy B, Kappel S, Wang J and Rogy MA: Interleukin-10-deficient mice and inflammatory bowel disease associated cancer development. Carcinogenesis 22: 665-671, 2001.
5. Matsuzaki K and Okazaki K: Transforming growth factor-beta during carcinogenesis: the shift from epithelial to mesenchymal signaling. J Gastroenterol 41: 295-303, 2006.
6. Moses HL, Yang EY and Pietenpol JA: TGF-beta stimulation and inhibition of cell proliferation: new mechanistic insights. Cell 63: 245-247, 1990.
7. MacDonald TT: Effector and regulatory lymphoid cells and cytokines in mucosal sites. Curr Top Microbiol Immunol 236: 113-135, 1999.
8. Maloy KJ and Powrie F: Regulatory T cells in the control of immune pathology. Nat Immunol 2: 816-822, 2001.
9. Eppert K, Scherer WS, Ozcelik H, *et al*: MADR maps to 18q21 and encodes a TGF-ß-regulated MAD-related protein that is functionally mutated in colorectal carcinoma. Cell 86: 543-552, 1996.
10. Zavadil J and Bottinger EP: TGF-ß and epithelial-to-mesenchymal transitions. Oncogene 24: 5764-5774, 2005.
11. De Caestecker MP, Piek E and Roberts AB: Role of transforming growth factor-ß signaling in cancer. J Natl Cancer Inst 92: 1388-1402, 2000.
12. Kolb M, Margetts PJ, Anthony DC, *et al*: Transient expression of IL-1beta induces acute lung injury and chronic repair leading to pulmonary fibrosis. J Clin Invest 107: 1529-1536, 2001.
13. Heldin CH, Miyazono K and ten Dijke P: TGF-ß signaling from cell membrane to nucleus through SMAD proteins. Nature 390: 465-471, 1997.
14. Derynck R and Zhang YE: Smad-dependent and Smad-independent pathways in TGF-ß family signaling. Nature 425: 577-584, 2003.
15. Saika S, Kono-Saika S, Ohnishi Y, *et al*: Smad3 signaling is required for epithelial-mesenchymal transition of lens epithelium after injury. Am J Pathol 164: 651-663, 2004.
16. Furukawa F, Matsuzaki K, Mori S, *et al*: p38 MAPK mediates fibrogenic signal through Smad3 phosphorylation in rat myofibroblasts. Hepatology 38: 879-889, 2003.
17. Mori S, Matsuzaki K, Yoshida K, *et al*: TGF-ß and HGF transmit the signals through JNK-dependent Smad2/3 phosphorylation at the linker regions. Oncogene 23: 7416-7429, 2004.
18. Yoshida K, Matsuzaki K, Mori S, *et al*: Transforming growth factor-ß and platelet-derived growth factor signal via c-Jun N-terminal kinase-dependent Smad2/3 phosphorylation in rat hepatic stellate cells after acute liver injury. Am J Pathol 166: 1029-1039, 2005.
19. Ekbom A, Helmick C, Zack M and Adami HO: Ulcerative colitis and colorectal cancer. A population-based study. N Engl J Med 323: 1228-1233, 1990.
20. Balkwill F and Mantovani A: Inflammation and cancer: back to Virchow? Lancet 357: 539-45, 2001.
21. Oft M, Peli J, Rudaz C, Schwarts H, Beug H and Reichmann E: TGF-beta1 and Ha-Ras collaborate in modulating the phenotypic plasticity and invasiveness of epithelial tumor cells. Genes Dev 10: 2462-2477, 1996.
22. Shi Y and Massague J: Mechanisms of TGF-beta signaling from cell membrane to nucleus. Cell 113: 685-700, 2003.
23. Derynck R and Zhang YE: Smad-dependent and Smad-independent pathways in TGF-beta family signaling. Nature 425: 577-584, 2003.
24. Kretschmar M, Doody J, Timokhina I and Massague J: A mechanism of repression of TGFbeta/Smad signaling by oncogenic Ras. Genes Dev 13: 804-816, 1999.
25. Robinson MJ and Cobb MH: Mitogen-activated protein kinase pathways. Curr Opin Cell Biol 9: 180-186, 1997.
26. Miyaki M and Kuroki T: Role of Smad4 (DPC4) inactivation in human cancer. Biochem Biophys Res Commun 306: 799-804, 2003.
27. Zhu Y, Richardson JA and Parada LF: Smad3 mutant mice develop metastatic colorectal cancer. Cell 94: 703-714, 1998.
28. Yamagata H, Matsuzaki K, Mori S, *et al*: Acceleration of Smad2 and Smad3 phosphorylation via c-Jun NH2-terminal kinase during human colorectal carcinogenesis. Cancer Res 65: 157-165, 2005.
29. Mulder KM: Role of Ras and Mapks in TGFbeta signaling. Cytokine Growth Factor Rev 11: 23-35, 2000.
30. Vogelstein B: Cancer. A deadly inheritance. Nature 348: 681-682, 1990.
31. Harpaz N, Peck AL, Yin J, *et al*: p53 protein expression in ulcerative colitis-associated colorectal dysplasia and carcinoma. Hum Pathol 25: 1069-1074, 1994.

Inducible expression of microRNA-194 is regulated by HNF-1α during intestinal epithelial cell differentiation

KIMIHIRO HINO,[1,2,3] KIICHIRO TSUCHIYA,[1,3] TARO FUKAO,[1] KOTARO KIGA,[1,2] RYUICHI OKAMOTO,[1] TAKANORI KANAI,[1] and MAMORU WATANABE[1]

[1]Department of Gastroenterology and Hepatology, Graduate School, Tokyo Medical and Dental University, Tokyo 113-8519, Japan
[2]Department of Chemistry and Biotechnology, Graduate School of Engineering, The University of Tokyo, Tokyo, 113-8656, Japan

ABSTRACT

Maintenance of the intestinal epithelium is based on well-balanced molecular mechanisms that confer the stable and continuous supply of specialized epithelial cell lineages from multipotent progenitors. Lineage commitment decisions in the intestinal epithelium system involve multiple regulatory systems that interplay with each other to establish the cellular identities. Here, we demonstrate that the microRNA system could be involved in intestinal epithelial cell differentiation, and that microRNA-194 (miR-194) is highly induced during this process. To investigate this inducible expression mechanism, we identified the genomic structure of the *miR-194-2, -192* gene, one of the inducible class of miR-194 parental genes. Furthermore, we identified its transcriptional regulatory region that contains a consensus-binding motif for hepatocyte nuclear factor-1α (HNF-1α), which is well known as a transcription factor to regulate gene expression in intestinal epithelial cells. By chromatin immunoprecipitation assay and luciferase reporter analysis, we revealed that pri-miR-194-2 expression is controlled by HNF-1α, and its consensus binding region is required for the transcription of pri-miR-194-2 in vivo in an intestinal epithelial cell line, Caco-2. Our observations indicate that microRNA genes could be targets of lineage-specific transcription factors and that microRNAs are regulated by a tissue-specific manner in the intestinal epithelium. Therefore, our work suggests that induced expression of these microRNAs have important roles in intestinal epithelium maturation.

Keywords: microRNA; miR-194; Caco-2; differentiation; HNF-1α; intestine

INTRODUCTION

The intestinal epithelial system is a paradigm for the production of distinct cell lineages from multipotent progenitors (Crosnier et al. 2006). The molecular mechanism of balanced and continuous generation of intestinal epithelial cells has been extensively investigated, as it would be involved in the pathogenesis of gastrointestinal disorders such as intestinal epithelial tumors. Recent studies highlighted the critical roles of specific signaling pathways directing activation of certain transcription factors, such as Notch and Wnt pathways, in the development of intestinal epithelium, clearly indicating that its developmental program is under the control of dynamic gene regulatory networks (Sancho et al. 2004; Fre et al. 2005; Gregorieff and Clevers 2005; Stanger et al. 2005; Clarke 2006; Crosnier et al. 2006).

microRNAs (miRNAs) are 21–23-nucleotide (nt) noncoding RNAs that function as post-transcriptional regulators of gene expression in various species (Ambros 2004; Bartel 2004; Zamore and Haley 2005). miRNAs recognize their target(s) with the partially complementary sequences and repress their translation or modify their stability (Olsen and Ambros 1999; Jing et al. 2005). miRNAs play essential roles in diverse events, including control of developmental timing (Wightman et al. 1993), differentiation (Chen et al. 2004, 2006; Esau et al. 2004; Kim et al. 2006), apoptosis, cell proliferation (Brennecke et al. 2003; Cheng et al. 2005; Cimmino et al. 2005), and organ development (Giraldez et al. 2005).

miRNAs initially appear as relatively long transcripts called pri-miRNA, and it is now widely accepted that many

[3]These authors contributed equally to this work.

Abbreviations: miRNA, microRNA; SI, sucrase-isomaltase; kb, kilobases; LPH, lactase-phlorizin hydrolase; HNF-1α, hepatocyte nuclear factor-1 α; PCR, polymerase chain reaction; RT, reverse transcription; RACE, rapid analysis cDNA end; MEM, minimal essential medium; DMEM, Dulbecco's modified Eagle's Medium; PBS, phosphate buffered saline; FBS, fetal bovine serum.

Reprint requests to: Mamoru Watanabe, Department of Gastroenterology and Hepatology, Graduate School, Tokyo Medical and Dental University, 1-5-45 Yushima, Bunkyo-ku, Tokyo 113-8519, Japan; e-mail: mamoru.gast@tmd.ac.jp; fax: 81-3-5803-0262.

Article published online ahead of print. Article and publication date are at http://www.rnajournal.org/cgi/doi/10.1261/rna.810208.

pri-miRNAs are transcribed by RNA polymerase II (Cai et al. 2004; Lee et al. 2004), suggesting that tissue- and time-specific expression of miRNAs is probably specified at the level of pri-miRNA transcription. Although hundreds of miRNAs were cloned in various species, the regulatory mechanisms of specific pri-miRNAs are still largely unknown. Studies regarding regulation of each pri-miRNA would therefore provide clues to the further understanding of miRNA biology in general or of particular functions in specific cell lineages.

In this study, we focused on the miRNA system as novel molecular machinery in intestinal epithelial cell differentiation. Our high-throughput miRNA expression profiling revealed a dynamic change of the miRNA expression pattern during Caco-2 differentiation, which is one of the most widely known intestinal epithelial differentiation models. In the model, we found that dozens of miRNAs were up- or down-regulated. Among such miRNAs, miR-194 was found to be highly up-regulated with tight tissue specificity. To know the precise regulatory mechanism, we determined the genomic structure of pri-miR-194-2. Given the genomic structure, we also identified a highly conserved genomic region close to the transcription start site of pri-miR-194-2 that contains a consensus binding motif for hepatocyte nuclear factor-1α (HNF-1α). Chromatin immunoprecipitation (ChIP) assay confirmed physical binding of HNF-1α to this conserved region in vivo, and other functional assays further showed the transcriptional role of HNF-1α for the pri-miR-194-2 transcription, suggesting that the conserved genomic region is the core promoter element for pri-miR-194-2 and that HNF-1α is the key transcription factor for the expression of this miRNA.

Because HNF-1α is one of the critical factors of intestinal epithelial gene expression during differentiation and maturation, miR-194 might constitute a certain part of its regulatory network, thereby contributing to the regulation of gene expression program in intestinal epithelial cells. Therefore, our work suggests that induced expression of miRNAs has an important role in intestinal epithelium maturation.

RESULTS

miR-194 is highly induced during intestinal epithelial cell differentiation

Adopting the differentiation system of intestinal epithelial cell line Caco-2, possible alteration of miRNA expression pattern during intestinal epithelial differentiation was examined. Induction of differentiation in Caco-2 cells was performed by conventional long-term confluent culture method. Following confirmation of maturation status by the differentiation markers such as lactase-phlorizin hydrolase (LPH) and sucrase-isomaltase (SI) (Fig. 1A), 156 mature miRNAs were quantified in differentiated and proliferative cells by the TaqMan-based high-throughput profiling method. As shown in Figure 1, B and C, several miRNAs were significantly up- or down-regulated during Caco-2 differentiation as judged by Ct values. Among such genes, expression of miR-133a and miR-133b has been previously detected in tissues other than intestine (Chen et al. 2006). Also, miR-146 has been reported to control Toll-like receptor and cytokine signaling (Taganov et al. 2006), whereas the miR-34 family has been shown to be involved in the p53 network (He et al. 2007). Inhibition of miR-148 and 210 increases the level of apoptosis, while inhibition of miR-152 decreases cell growth (Cheng et al. 2005). Consequently, differentially expressed miRNAs observed in the present experiment suggested that miRNA machineries that control general physiological events are involved in epithelial cell differentiation.

Although identification of sets of miRNA as regulators of general events is important, here, we rather sought to find some miRNAs that are regulated specifically in intestinal epithelial cells. Among differentially expressed miRNAs, miR-194 was one of the highly induced miRNAs during differentiation and showed the highest intensity in differentiated Caco-2 cells (Fig. 1D). Induction of mature miR-194 upon Caco-2 differentiation was also confirmed by Northern blot (Fig. 1E). Also, tissue distribution of mature miRNA-194 in an adult mouse was identified to be relatively specific in intestinal tracts (Fig. 1F), consistent with some previous results in other organisms such as zebrafish embryo (Wienholds et al. 2005).

These data collectively suggested that, among numerous regulated miRNAs, miRNA-194 is highly and specifically induced in intestinal epithelial cells during its differentiation.

Genomic structures of miR-194 primary transcripts

Given the high and specific expression of miR-194 in intestinal epithelial cells, we further sought to characterize this miRNA to know its regulation. According to miRBase, mature miR-194 can be derived from two separate loci on human genome that are registered as *miR-194-1* and *miR-194-2* (Fig. 2A). The miR-194-1 and miR-194-2 are encoded on human chromosomes 1 and 11, respectively. As like many other miRNAs, both miR-194-1 and miR-194-2 are so-called clustered miRNA and have cluster partners miR-215 and miR-192, respectively.

To examine whether either of the two loci can generate mature miR-194, we constructed miRNA expression vectors in which miR-194 loci were inserted downstream of the CMV promoter, and observed mature miR-194 generation using luciferase sensor reporter assay. As luciferase sensor mRNA have perfect complementary sequence against mature miR-194 in 3′UTR, if mature miR-194 is generated from the miR-194 loci, firefly sensor mRNA is cleaved by RNAi effect. Thus, miRNA generation could be observed as reduction of luciferase activity.

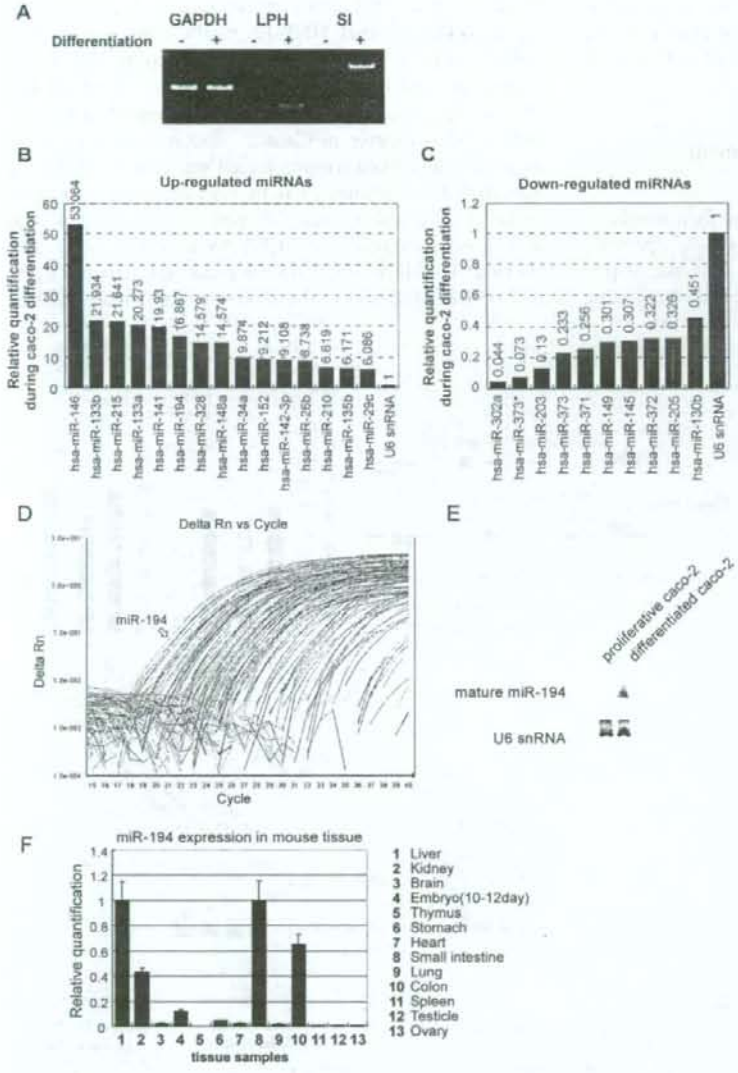

FIGURE 1. Altered expression profile of miRNA during Caco-2 differentiation. (*A*) Detection for differentiation markers by RT-PCR. RT-PCR was performed on total RNAs extracted from proliferative or differentiated Caco-2 cells. PCR products were separated by 5% acrylamide gel electrophoresis and stained by EtBr. (*B*) Up-regulated miRNAs during Caco-2 differentiation. A total of 156 miRNAs were quantified by TaqMan miRNA assays Human Panel–Early Access Kit. Relative Quantification (RQ) was normalized by U6 RNA endogenous control. Quantification results were arranged by RQ and cut-off detectors whose Ct values were more than 30 cycles in differentiated Caco-2 cells. (*C*) Down-regulated miRNAs during Caco-2 differentiation, observed in the quantification performed in *B*. (*D*) Amplification plot by TaqMan miRNA assay in differentiated Caco-2 cells. Arrow indicates amplification plot of miR-194. (*E*) Northern blot of mature miR-194. Total RNAs (30 μg) were separated in 8 M urea 12% PAGE and transferred to Nybond N+. After UV cross-linking, the membrane was hybridized with DIG-labeled RNA probe. Hybridized probes were detected by AP-conjugated anti-DIG antibody and visualized by CDP-star. (*F*) miR-194 expression in various mouse tissues. Expression of miR-194 was quantified by TaqMan miRNA assay. U6 snRNA was used as endogenous control. The expression level in small intestine was set to 1.

Forced expression of each locus showed marked decrease of the sensor luciferase activity in both Hela S3 and Caco-2 cells (Fig. 2B). As the results of this assay showed that both loci are able to generate mature miR-194, we sought to examine which locus is the origin of miR-194 that is induced upon differentiation of intestinal epithelial cells. Northern blot analysis of pre-miRNAs showed up-regulation of both pre-miRNAs (Fig. 2C), whereas TaqMan miRNA assay showed up-regulation of miR-194, miR-192, and miR-215 upon Caco-2 differentiation (Fig. 2D). Quantitative RT-PCR using a reverse-transcribed sample as a standard template also showed induction of pri-miRNA from both loci upon differentiation, but a relatively higher induction of pri-miR-194-2 was observed, compared with pri-miR-194-1 (Fig. 2E, left). Absolute quantification using genomic DNA as a standard template, which enables quantitative comparison between pri-miR-194-1 and pri-miR-194-2, also demonstrated that expression of pri-miR-194-2 was more abundant in differentiated Caco-2 cells, compared with pri-miR-194-1 (Fig. 2E, right).

Having these observations, we focused on miR-194-2 cluster and further characterized this locus. Upon the database search, a registered cDNA, AK092802, was found as a putative 5′ part of the pri-miR-194-2 transcript (Fig. 3A). As shown by RT-PCR, the registered transcript AK092802 and the region encoding pre-miR-194-2 were transcribed primarily as a single RNA (Fig. 3B). Also, the 5′ region of the transcript including the transcription start site of pri-miR-194-2 was determined by 5′ RACE. Although 5′ RACE presented two fragments, sequence analysis revealed that these two fragments arise from the same transcription start site, while the difference in length was due to splicing (Fig. 3C). Furthermore, we performed 3′ RACE to identify the structure of pri-miR-194-2, -192 (Fig. 4A). The identified pri-miRNA shared the same 3′ terminal with that of another registered transcript, AW207381 (Fig. 4B), and induced